

Institut für Veterinärpathologie, Abteilung für Infektionspathologie  
der Vetsuisse-Fakultät Universität Zürich

Direktorin Institut: Prof. Dr. med. vet., Dipl.ECVP Anja Kipar  
Leiterin Abteilung: Prof. Dr. med. vet., Dipl.ECVP, Nicole Borel

Arbeit unter wissenschaftlicher Betreuung von  
Prof. Dr. med. vet., Dipl.ECVP, Nicole Borel

Elucidating the histologic findings of *Chlamydia pecorum*- induced arthritis in sheep

### **Inaugural-Dissertation**

zur Erlangung der Doktorwürde der  
Vetsuisse-Fakultät Universität Zürich

vorgelegt von

**Nina Ostfeld**

Tierärztin  
aus Bremen, Deutschland

genehmigt auf Antrag von

Prof. Dr. med. vet., Dipl.ECVP, Nicole Borel, Referentin  
Prof. Dr. med. vet. Michael Hässig, Korreferent

**2020**





## Index

<b>1 SUMMARY .....</b>	<b>4</b>
<b>2 ZUSAMMENFASSUNG .....</b>	<b>5- 6</b>
<b>3 THESIS .....</b>	<b>7- 42</b>
<b>ABSTRACT .....</b>	<b>9- 10</b>
<b>INTRODUCTION .....</b>	<b>10- 11</b>
<b>MATERIALS AND METHODS .....</b>	<b>11- 17</b>
<b>RESULTS .....</b>	<b>17- 22</b>
<b>DISCUSSION .....</b>	<b>22- 27</b>
<b>CONCLUSIONS.....</b>	<b>27- 28</b>
<b>ACKNOWLEDGEMENTS.....</b>	<b>28</b>
<b>DECLARATION OF CONFLICTING INTERESTS.....</b>	<b>28</b>
<b>FUNDING .....</b>	<b>29</b>
<b>REFERENCES .....</b>	<b>29- 37</b>
<b>FIGURE LEGENDS.....</b>	<b>38- 42</b>
<b>ANNEXES .....</b>	<b>43- 78</b>
<b>TABLES 1-7 .....</b>	<b>43- 54</b>
<b>FIGURES 1-31.....</b>	<b>55- 63</b>
<b>SUPPLEMENTARY TABLES 1-4.....</b>	<b>64- 77</b>
<b>4 DANKSAGUNG</b>	
<b>5 CURRICULUM VITAE</b>	

**Elucidating the histologic findings of *Chlamydia pecorum*- induced arthritis in sheep**

*Chlamydia pecorum* is an obligate intracellular pathogen with a wide host range such as sheep, cattle, goats and pigs as well as koalas. Chlamydial polyarthritis is the economically most important infection in young sheep. In the present study, tissues from experimentally and naturally *Chlamydia pecorum* infected sheep, were assessed histologically and immunohistochemically. Tissues of joints and inner organs of 35 sheep from different inoculation groups and of 5 naturally- infected lambs were investigated. Two different *C. pecorum* strains (IPA and E58), different routes of administration (intra-articular or intravenous), UVA- irradiated IPA strains, non-infected control groups and naturally infected sheep were compared. The most obvious inflammatory lesions were observed in joints and, interestingly, in the renal pelvis from both, experimentally and naturally infected animals. This resulted in chronic or chronic-active arthritis and pyelitis and intralesional chlamydial inclusions demonstrated by immunohistochemistry.

Immunohistochemical evaluation of the presence and distribution of macrophages, T and B cells in joints revealed macrophages. Previous observations indicated that *C. pecorum* isolates can infect circulating monocytes. Histological lesions in joints and inner organs and the presence of *C. pecorum* DNA, suggest chlamydial arthritis in lambs is the result of a systemic, hematogenous spread of *C. pecorum*.

**Key Words:** *Chlamydia pecorum*, arthritis, histopathology, immunohistochemistry, immune cells

**Untersuchung histologischer Befunde in *Chlamydia pecorum* – induzierter Arthritis beim Schaf**

*Chlamydia pecorum* ist ein obligat intrazelluläres Bakterium mit grossem Wirtsspektrum, einschliesslich Schafe, Rinder Ziegen, Schweine und Koalas. Durch Chlamydien verursachte Polyarthritiden bei Lämmern ist von grosser wirtschaftlicher Bedeutung. In der vorliegenden Studie wurden Gewebeproben von Gelenken und inneren Organen experimentell und natürlich infizierter Tiere (n=40) histologisch und immunhistologisch untersucht. Es wurden zwei verschiedene *C. pecorum*- Stämme (IPA und E58), verschiedene Verabreichungsformen (intraartikulär und intravenös), UVA- bestrahlte IPA Stämme, die nicht infizierte Kontrollgruppe und natürlich infizierte Schafe miteinander verglichen. Die deutlichsten entzündlichen Veränderungen fanden sich in den Gelenken und Nierenbecken experimentell und natürlich infizierter Tiere. Dabei fanden sich chronische oder chronisch- active Arthritiden und Pyelitiden, sowie Nachweise von Chlamydien- Antigen mittels Immunhistochemie.

Die immunhistologische Untersuchung des Auftretens und der Verteilung von Entzündungszellen (Makrophagen, T- und B- Zellen) und deren Verteilungsmuster, zeigte ein deutlich gehäuftes Auftreten von Makrophagen. Frühere Studien belegen die Fähigkeit von *C. pecorum*, zirkulierende Monozyten zu infizieren. Die histologischen Veränderungen in Gelenken und inneren Organen sowie der

56 Nachweis von *C. pecorum* DNA, unterstreicht die Annahme einer systemischen,  
57 hämatogenen Streuung.

58 **Schlüsselwörter:** *Chlamydia pecorum*, Arthritis, Histopathologie, Immunzellen,  
59 Immunohistochemie

60

61

62

63

64

65

66

67

68

69

70

71

72

73

74

**Elucidating the histologic findings of *Chlamydia pecorum*-induced arthritis in sheep**

**Ostfeld N.<sup>1</sup>, Islam M.M.<sup>2,3</sup>, Jelocnik M.<sup>2</sup>, Hilbe M.<sup>1</sup>, Sydler T.<sup>1</sup>, Hartnack S.<sup>4</sup>,  
Jacobson C.<sup>5</sup>, Clune T.<sup>5</sup>, Marsh I.<sup>6</sup>, Sales N.<sup>6</sup>, Polkinghorne A.<sup>7,8</sup>, Borel N.<sup>1</sup>**

<sup>1</sup>Institute for Veterinary Pathology, Vetsuisse Faculty, University of Zurich,  
Winterthurerstrasse 268, 8057 Zurich, Switzerland

<sup>2</sup>University of The Sunshine Coast, Genecology Research Centre, University of the  
Sunshine Coast, Sippy Downs 4557, Australia

<sup>3</sup>Department of Pathology and Parasitology, Faculty of Veterinary and Animal  
Science, Hajee Mohammad Danesh Science and Technology University, Dinajpur-  
5200, Bangladesh

<sup>4</sup>Section of Epidemiology, Vetsuisse Faculty University of Zurich,  
Winterthurerstrasse 270, 8057 Zurich, Switzerland

<sup>5</sup>College of Science, Health, Engineering and Education, Murdoch University, Perth,  
Western Australia 6150, Australia

<sup>6</sup>NSW Department of Primary Industries, Elizabeth Macarthur Agricultural Institut,  
Menangle, New South Wales 2568, Australia

<sup>7</sup>Department of Microbiology and Infectious Diseases, Nepean Hospital, NSW Health  
Pathology, Penrith 2750, New South Wales, Australia

<sup>8</sup>Nepean Clinical School, University of Sydney Medical School, University of Sydney,  
Penrith 2750, New South Wales Australian

96    **Corresponding author:** Prof. Dr. Dipl. ECVP Nicole Borel, Institute of Veterinary  
97    Pathology, Vetsuisse Faculty, University of Zurich, Winterthurerstrasse 268, CH-  
98    8057 Zurich, Switzerland. Email: N.Borel@access.uzh.ch. Telephone:  
99    0041446358563

100

## Abstract

*Chlamydia pecorum* is an obligate intracellular pathogen with a wide host range including livestock such as sheep, cattle, goats and pigs as well as wildlife species such as koalas. Chlamydial polyarthritis is the economically most important infection resulting in swollen joints, lameness, stiffness and weight loss in young sheep. In the present study, tissues from either *Chlamydia pecorum* experimentally or naturally infected sheep, were assessed histologically and immunohistochemically. In total, 312 tissues of carpal, hock and stifle joints as well as spleen, liver, kidney, lymph nodes, lung, conjunctiva and brain of 35 sheep from different inoculation groups and of naturally- infected lambs were investigated. Two different *C. pecorum* strains (IPA and E58), different routes of administration (intra-articular or intravenous), UVA-irradiated IPA strains, non-infected control groups and naturally infected sheep were compared. The most obvious inflammatory lesions were observed in joints and, interestingly, in the renal pelvis from the experimentally infected group and naturally infected animals. This resulted in chronic or chronic-active arthritis and pyelitis and intralesional chlamydial inclusions demonstrated by immunohistochemistry.

Immunohistochemical evaluation of the presence and distribution of macrophages, T and B cells in joints revealed macrophages as the most prevalent inflammatory cell population. Previous observations indicated that *C. pecorum* isolates can infect circulating monocytes. Together with the finding of the histological lesions in joints and inner organs alongside the presence of *C. pecorum* DNA, these observations suggest chlamydial arthritis in lambs is the result of a systemic, hematogenous spread of *C. pecorum*.

**Key Words:** *Chlamydia pecorum*, arthritis, infection model, lambs, histopathology,

125 immunohistochemistry, immune cells

## 126 **Introduction**

127 *Chlamydia (C.) pecorum* is a gram-negative, obligate intracellular bacterium with a  
128 broad host range including livestock such as sheep, cattle, goats and pigs as well as  
129 wildlife species like koalas.<sup>7,17,52</sup> Infection with *C. pecorum* can present with clinical  
130 manifestations such as arthritis, conjunctivitis, infertility, enteritis, endometritis,  
131 vaginitis, pneumonia, mastitis as well as sporadic bovine encephalomyelitis (SBE) in  
132 cattle.<sup>23,37,43,50,51</sup> The most important economical manifestation of *C. pecorum*,  
133 mainly prevalent in Australia and New Zealand, is polyarthritis in sheep which  
134 causes swollen joints, lameness, stiffness and weight loss in lambs.<sup>50</sup> Moreover, it is  
135 hypothesized, that the agent also infects the gastrointestinal tract of lambs  
136 asymptotically.<sup>13</sup> In Australian sheep flocks, prevalence of gastrointestinal  
137 shedding of >30% has been reported.<sup>53</sup>

138 Recent studies have used comparative genomics and molecular typing to identify  
139 differences in strain virulence.<sup>23,25,1,41</sup> It was shown that polyarthritic sheep had  
140 unique sequence types (e.g. ST23) when compared to rectally shed *C. pecorum*  
141 strains (e.g. ST62, ST63, ST81).<sup>1</sup>

142 The research group of Storz described polyarthritis in feeder lambs due to a PLGV  
143 agent (psittacosis-lymphogranuloma venerum agent) in the USA in the 1960's.<sup>46,47</sup>  
144 The agent induced inflammatory changes in synovial membranes and had the ability  
145 to pass the synovia/blood barrier followed by entry into the blood stream and causing  
146 mild inflammatory reactions in internal organs. Experimentally infected sheep  
147 showed identical pathological changes to those observed in naturally infected sheep  
148 recovering from PLGV-induced polyarthritis.<sup>46</sup> These early infection studies were



recently reproduced by Australian researchers.<sup>22</sup> While these experimental studies<sup>46,47,22</sup> focussed on clinical signs and gross findings due to *C. pecorum* infection in lambs, limited information is available on the histopathomorphological changes in infected animals. Therefore, the aim of our study was to examine joints and inner organs histologically and immunohistochemically by using specific quantitative and semiquantitative scoring systems. The use of such scoring systems might standardize and better characterize the pathogenesis of *C. pecorum*-induced arthritis in sheep and other arthritic diseases.

## **Materials and Methods**

### *Ethics statement*

This study was carried out in accordance with the New South Wales (NSW) Animal Research Act (1985) and Animal Research Regulation (2010); Australian Code for the Care and Use of Animals for Scientific Purposes. The protocol was considered and approved by the University of the Sunshine Coast Animal Ethics Committee (AN/S/18/56) and the Elizabeth Macarthur Agricultural Institute (EMAI) Animal Ethics Committee (M17/09). Animals were housed in Quarantine Containment Level 2 facilities at the Elizabeth Macarthur Agricultural Institute (EMAI) and veterinary procedures were carried out by qualified veterinarians. Naturally infected sheep were part of a project approved and monitored by Murdoch University Animal Ethics Committee (R3004/17).

*Experimental setup and groups, sample collection, histologic and PCR examination*

The experimental design was implemented during a previous study<sup>22</sup> and consisted of 35 Australian Merino sheep, 6 - 7 months of age and originating from a flock without any history of arthritis or *Chlamydia*-related health problems. These 35 sheep were selected following two rounds of prescreening for *Chlamydia* in over 100 sheep, collecting rectal swabs for a *C. pecorum*-specific qPCR as well as blood samples for complement fixation test (CFT).<sup>4</sup> Both tests confirmed *Chlamydia*-negative status in the 35 animals selected for experimental studies. All 35 sheep were weighed and randomly assigned to four groups: 1) IPA-group (n=10), 2) E58-group (n=10), 3) UV-irradiated IPA-group (n=10) and 4) control group (n=5). The infection groups received 10<sup>7</sup> inclusion forming units (IFU) of *C. pecorum* E58 or IPA strain either into the right carpal joint via the intra-articular route (IA; n=5 per group) or intravenously (IV; n=5 per group). The control group (n=5) received Sucrose Phosphate Glutamate (SPG) by the IA route (n=5). The *C. pecorum* IPA isolate used in this study originated from the joint of a sheep suffering from polyarthritis in the USA, while the E58 is also a USA isolate but was retrieved from the brain of a calf suffering from sporadic bovine encephalomyelitis.<sup>33</sup>

Euthanasia, necropsy and tissue sampling were performed at various time points (Table 1) after the administration of the inoculum as described previously.<sup>22</sup> Tissues of carpal, hock and stifle joints and from the following inner organs: kidney, liver, spleen, lungs, lymph nodes and brains from experimentally infected animals were collected in 10% formalin and processed as previously described.<sup>22</sup>

In an additional study, five sheep (3619, 7578, 7629, 8084, 8452), approximately six months of age, from a commercial farm approximately 165 km south-east of Perth,

Australia, were assessed as having swollen joints and chronic lameness. One sheep also had evidence of conjunctivitis at the time of examination. Sheep were euthanized via intravenous barbiturate overdose. Tissues of left and right carpal joint, liver, kidney, mesenteric lymph node and lung were collected from these naturally infected animals, fixed using 10% formalin and processed as previously described.<sup>22</sup> Samples of spleen were collected for all sheep except number 8084. In addition, tissues of the right stifle joint, the left conjunctiva and third eyelid from animal number 3619 were available. Sterile dry swabs were used to sample synovia (carpus) and screened for *Chlamydia* with the previously described *C. pecorum*-specific qPCR.<sup>26</sup> This confirmed the presence of *C. pecorum* DNA in joints (synovia) for all five sheep (5/5).

In total, 110 formalin-fixed and paraffin-embedded (FFPE) tissue blocks deriving from experimentally inoculated sheep (n=35) and naturally infected animals (n=5) were included in this study. Hematoxylin and eosin (HE) stained slides were prepared from all tissues according to standard procedures.

To detect chlamydial DNA, qPCR was performed on the joint tissues of both experimentally and naturally infected animals and the organs of only the experimentally infected animals. Positive qPCR results were listed per group, organ or joint and were compared against each other considering copies per microliter.

### *Joints*

From experimentally infected animals, a total of 32 slides from carpal, hock and stifle joints were examined (Supplemental Table S1). From naturally infected animals (n=5), a total of 12 slides from carpal, hock and stifle joints (10/12 carpal joints and

2/12 stifle joints) were investigated (Supplemental Table S2). The assessment was performed by two pathologists in a blinded manner (at a magnification of 100x and 400x) by using a light microscope (Leitz, Laborlux S, Germany) and pathological diagnoses were elaborated. Five main microscopic findings, focussing on inflammation, were identified and assessed qualitatively: The presence of inflammation, the type of inflammation, the degree and distribution of inflammation and whether the surrounding tissue was affected or not (Fig. 1). Then, inflammatory joint lesions were evaluated according to semi-quantitative parameters resulting in a newly developed scoring system with a maximum reachable score of 48 per animal (Table 2). In addition to parameters described in Fig. 1, the scoring system also included important findings such as the presence of fibrin and granulation tissue and positive immunolabeling for *Chlamydiaceae*. Furthermore, the synovia was evaluated according to criterias as previously described<sup>10,15,28</sup> and total scores per experimental group were evaluated (Table 3).

### *Inner organs*

From experimentally infected animals, a total of 72 slides from inner organs (livers, kidneys, brains, spleen, lymph nodes and lungs) were examined. From naturally infected animals (n=5), a total of five slides were examined from inner organs while only 1/5 conjunctival tissues were investigated. The assessment was performed by two pathologists in a blinded manner (at a magnification of 100x and 400x) by using a light microscope (Leitz, Laborlux S, Germany) and pathological diagnoses were elaborated (Supplemental Table S3). The four main microscopic findings of inflammation were identified and assessed qualitatively: these were the presence of inflammation, the type, degree and the distribution of inflammation (Fig. 2).

Inflammatory lesions of inner organs were also evaluated according to semi-quantitative parameters, resulting in a newly developed scoring system with a maximum reachable score of 39 per animal (Table 4). In addition to the parameters described in Fig. 2, the scoring system also included the presence of positive immunolabeling for *Chlamydiaceae*.

For lung tissues, high-resolution digital scans were acquired using the Hamamatsu Photonics's NanoZoomer HT2.0 (Hamamatsu, Japan). All bronchi and bronchioli per lung section were measured and for those with a minimal diameter of 200 micrometer, peribronchial and peribronchiolar lymph follicles (representing BALThyperplasia) and other lymphocytic accumulations were assessed.

Lymph nodes and spleen were analyzed for the presence of hyperplasia as previously described.<sup>3</sup> The area of the whole tissue on each section was measured, the number of follicles were counted at a magnification of 100x and assessed semiquantitatively using a newly developed scoring system (0 = 10, 1 = >20, 2 = >50, lymph follicles per section and 0 = 1-4, 1 = 5-10, 2 = >10 secondary follicles with germinal centers). For lymph nodes and spleen, a minimum of five randomly chosen slides per each group was examined in a blinded manner. All tissue assessments were performed according to the targeted masked review, as previously described.<sup>31</sup>

### *Immunohistochemistry*

Immunohistochemistry (IHC) to detect chlamydial antigen in tissues of joints and inner organs of experimentally infected, naturally infected and control animals was performed as previously described.<sup>22</sup> A total of 248 IHC sections were examined using a light microscope (Leitz, Laborlux S, Germany) at a magnification of 100x and

400x. A positive immunohistochemistry signal was included into the scoring system (Supplemental Table S1, S2 and S3, Table 2 and 4). IHC was considered positive if an intracytoplasmic granular labeling in at least one cell (organ-specific) was present.

FFPE joint sections (n=45) were re-evaluated for the presence and percentage of inflammatory cells (macrophages, B and T cells) by immunohistochemical labeling to detect Iba1 (macrophages), CD20 (B cells) and CD3 (T cells) antigens. Briefly, the sections were mounted on positively charged slides and dried overnight at 37°C. After deparaffinization, different antigen demasking protocols for each antibody were applied (Table 5). For the semi-quantitative evaluation, areas with inflammatory infiltrations were first selected in HE stained slides at 100x magnification. Then, the percentage of IHC-positive labelled cells (ranging from 0-100%, in 5 % steps) was counted in five randomly selected regions in corresponding IHC-slides for Iba1, CD20 and CD3 at 400x magnification.

### *Statistical analysis*

Statistical analyses were performed on data from experimentally infected animals and the corresponding control group using the software R <sup>40</sup> version R3.6.3. Generalized mixed effect models with a poisson distribution were performed using the lme4 package to evaluate the results of histological assesement of joint and inner organ lesions using the newly developed scoring system.<sup>2</sup> Because liver lesions were only mild and also present in control and UV-irradiated groups, we can assume that they were not related to the *C. pecorum* infection and were therefore excluded from the statistical evaluation. As fixed effects, group and joints or organs,

and as random effects, animals were considered. To adjust for multiple comparisons, Dunnett's or Tukey's approach containing the package multcomp<sup>18</sup> were chosen.

In lung tissues, bronchioli with a minimal diameter of 200 micrometer were assessed for peribronchiolar lymphocytic accumulation and lymph follicles (representing BALT-hyperplasia). Lymph nodes and spleen were analyzed for the presence of hyperplasia by the assessment of lymph follicles as well as secondary follicles using a newly developed scoring system in consideration of the area-size of each tissue section. Linear models were used for the evaluation of lung tissues and tissues of spleen and lymph nodes. The measurements of the biomarkers (CD3, CD20, Iba1) were dichotomized into absence and presence and the proportion of present biomarkers was described with Wilson's binomial 95% confidence intervals using the package, DescTools.<sup>45</sup> Generalized estimation equations were used to assess if the biomarkers differed between the experimental groups and locations by using the package, geepack.<sup>19</sup> The qPCR measurements in the joints and organs were analyzed with mixed poisson and zero-inflated poisson models using the packages lme4<sup>2</sup> and glmmTMB.<sup>8</sup>

## Results

### *Histologic findings in joints*

Joints of animals from control and IPA UV-irradiated groups did not show any signs of inflammation. In joints of experimentally infected animals, the majority of inflammatory lesions were chronic (lymphoplasmahistiocytic including granulation tissue) (Fig. 3, 4), followed by chronic-active (lymphoplasmahistiocytic and purulent including fibrin accumulations) arthritis/synovitis (Fig. 5, 6). Six of the evaluated joints

(n=94) showed an acute arthritis/synovitis. According to the semi-quantitative parameters in the scoring system, the most severe histological joint lesions were observed in the IPA i.v. group, followed by the E58 i.a. group. Moderate inflammatory changes were seen in the IPA i.a. group, followed by mild lesions in the joints of the E58 i.v. group (Table 6). Additional findings (synoviocyte proliferation, neovascularisation and periarterial fibrosis) (Table 3) were evaluated and the IPA i.v. group had the highest number of animals (14/20) which showed one or more of these pathological lesions (Fig. 7, 8). Stifle joints had the highest score followed by carpal and hock joints (Supplemental Table S4). An investigation of joint pathology score differences between the experimental groups and the control group were analyzed using generalized mixed effect models with a poisson distribution. The groups E58 i.a., IPA i.v. and IPA i.a. differed significantly from the control group (Supplemental Table S5). In joints of naturally infected animals, 5/5 animals had inflammatory lesions. The majority of inflammatory lesions were chronic-active processes (lymphoplasmahistiocytic and purulent arthritis/synovitis) (Fig. 9, 10). The right carpus of animal number 7629 did not show any inflammatory signs.

#### *Histologic findings in inner organs*

The brains of animals from the control and IPA UV-irradiated groups did not show any signs of inflammation. In brains of the experimentally infected animals, the most obvious inflammatory lesion was a mild chronic lymphohistiocytic (meningo-) encephalitis (5/20 animals) (Table 7, Fig. 11). In 3/35 brains (UVA-IPA i.a.: n=1, E58 i.v.: n=1, IPA i.v.: n=1), glia nodules were present (Fig. 11, insert). In these cases, by examination of brain sections following immunohistochemistry, a toxoplasmosis



infection was assessed (immunohistochemistry for detection of *T. gondii* using the rabbit polyclonal antibody RB-282-A0, Thermo Fisher Scientific; dilution 1:50) with negative results.

Lung tissues from all experimental animals (n=35) did not reveal any signs of inflammation, thus no significant differences were found between the groups. BALT hyperplasia was present in 23/35 lungs in animals from all groups (Fig. 12). Secondary follicles were found in 28/35 lymph nodes in animals from all groups (Fig. 13).

A mild chronic multifocal periportal hepatitis was present in 5/15 livers of animals from the control and the IPA UV-irradiated groups (Fig. 14). Similar lesions were also observed in 8/20 livers of animals in the other experimentally infected groups. Occasional leukocytostasis in liver vessels was present in all groups (Table 7).

The control and IPA UV-irradiated groups did not exhibit any lesions in the kidneys (Table 7). In other groups of infected animals, the most obvious kidney lesion was a chronic or chronic-active pyelitis, which partially ascended into the interstitium and was most severe in the IPA i.v. group (Fig. 15, 16). Statistical analyses of differences between the experimental groups compared to the control group revealed significant differences in group IPA i.v. (Supplemental Table S5).

Tissues of spleen and lymph nodes from all experimentally infected animals (n=35) did not reveal any signs of inflammation and no significant differences were found (Supplemental Table S4). For the investigation of differences between the experimental groups compared to the control group in lymph nodes, linear model measurement was performed and revealed a significant difference ( $p < 0.08$ ) between numbers of follicles in the E58 i.v. group compared to the control group but

no significant differences regarding the numbers of secondary follicles  
(Supplemental Table S5).

In naturally infected animals, lungs, lymph nodes and spleen did not show any  
inflammatory lesions. A mild chronic multifocal periportal hepatitis was present in  
livers of all animals (n=5). In 5/5 animals, a chronic (animals number 3619 and 7629)  
or chronic-active (animals number 8452, 7578 and 8084) pyelitis, which partially  
ascended into the interstitium, was seen (Fig. 17). A severe chronic  
(lymphoplasmahistiocytic) multifocal conjunctivitis was seen in animal number 3619  
(Fig. 18).

#### *Immunohistochemistry*

Immunohistochemical labeling for detecting chlamydial antigen in experimentally  
infected animals revealed positive results in the carpal joint of animal 628 from the  
IPA i.a. group, in the stifle joint of animal 658 from the IPA i.v. group, in carpal, hock  
and stifle joint of animal 710 from the E58 i.a. group and in the kidney of animal 616  
from the IPA i.v. group (Fig. 19, 20).

In naturally infected animals, immunohistochemical labeling for detecting chlamydial  
antigen revealed positive results in the left and right carpal joint of animal number  
3619 (Fig. 21), in the right carpal joint and kidney of animal 7578 (Fig. 22), the left  
carpal joint of animal number 7629, the right carpal joint of animal number 8084 and  
the kidney of animal number 8452.

Immunohistochemical labeling in experimentally infected animals to detect Iba1  
(macrophages, Fig. 23), CD20 (B cells, Fig. 24) and CD3 (T cells, Fig. 25) antigens  
was histologically most obvious for detecting macrophages (iba1). The same pattern

was observed in the five naturally infected animals using antibodies against Iba1 (Fig. 26), CD20 (Fig. 27) and CD3 (Fig. 28). For the immunohistological labeling (Iba1, CD20, CD3) in experimentally infected animals, a statistical evaluation was performed. Wilson's binomial 95% confidence intervals revealed the highest proportions in positive stained cells for Iba1 labeling (7.39), followed by CD20 (3.12) and CD3 (1.80) with the highest amount in carpal joints (170), followed by stifle (160) and hock joints (155). For CD3 labeling, the groups IPA i.a., IPA i.v. and E58 i.a. differed significantly from the control group with the highest presence in carpal joints followed by stifle and hock joints (Supplemental Table S5, Fig. 29). CD20 labeling revealed a significant difference in the E58 i.a., IPA i.a. and IPA i.v. group when compared to the control group with the highest presence in carpal joints followed by stifle and hock joints (Supplemental Table S5, Fig. 30). For Iba1 labeling, the groups E58 i.a., IPA i.v. and IPA i.a. group differed significantly from the control group with the highest presence in carpal joints followed by stifle and hock joints (Supplemental Table S5, Fig. 31).

#### *qPCR results*

By qPCR, 8/15 joint tissues from the IPA i.a. group were positive for chlamydial DNA (5/5 carpal joints, 1/5 hock joint and 2/5 stifle joints) with a range of 71 to 142'313 copies/μl. In the IPA i.v. group, 11/15 joint tissues were tested positive for chlamydial DNA (qPCR, 2/5 carpal joints, 5/5 hock joint and 4/5 stifle joints) with a range of 130 to 2506 copies/μl. In the E58 i.a. group, 5/15 tissues of carpal joints were positive for chlamydial DNA via qPCR with a range of 9641 to 167'349 copies/μl and in the E58 i.v. group, 8/15 joint tissues were positive (qPCR, 2/5 carpal joints, 4/5 hock joint and 2/5 stifle joints) with a range of 92 to 1884 copies/μl. Wilson's binomial 95%

confidence intervals revealed the highest proportions in carpal joints followed by stifle and hock joints (Supplemental Table S4). This was also confirmed by mixed poisson and zero-inflated poisson models. The groups which received intra-articular inoculation differed significantly from the intravenously inoculated groups (Supplemental Table S5). In carpal, hock and stifle joints, the highest qPCR loads (copies/ $\mu$ l) were evaluated in the IPA i.a. group (Supplemental Table S4, loads per joints and groups). Regarding the inner organs, Wilson's binomial 95% confidence intervals revealed the highest proportions of qPCR loads in lymph nodes, followed by liver, brain, kidney, spleen and lung (Supplemental Table S4). Mixed poisson and zero-inflated poisson models revealed a significant difference in the qPCR load of the lungs. The analysis revealed no significant differences between the groups (Supplemental Table S5). In brains, kidneys, livers and lungs, maximal qPCR loads (copies/ $\mu$ l) were evaluated in the E58 i.v. and in the IPA i.v. groups in lymph nodes (Supplemental Table S4, loads per organs and groups). In naturally infected animals, 4/5 joint tissues (left hock of animal number 3619, left carpus of animal number 7629, right carpus of animal number 7579 and right carpus of animal number 3619) were positive for chlamydial DNA with a range of 6.76 to 163 copies/ $\mu$ l.

## Discussion

*Chlamydia pecorum*-associated arthritis in sheep is an economically important infectious disease in Australia causing losses to the sheep industry.<sup>50</sup> In this study, we investigated histomorphological lesions of joints and inner organs from experimentally and naturally infected sheep to elucidate the pathogenesis of *C. pecorum*-associated arthritis. Tissue samples were retrieved from an experimental

challenge model in sheep.<sup>22</sup> This challenge model evaluated two different inoculation routes (intraarticular, intravenous) and the disease progression of two virulent *C. pecorum* isolates (E58, IPA). The challenge study focussed on clinical outcomes and gross pathology lesions with the aim of establishing an infection model that can be utilized in the future for potential vaccine validation. *C. pecorum* E58 was isolated from the brain of a calf with Sporadic Bovine Encephalomyelitis<sup>33</sup> whereas *C. pecorum* IPA originated from a joint of a polyarthritic sheep.<sup>35</sup> Both strains were able to establish systemic infections as shown in previous studies<sup>46,47</sup> and also confirmed in this study.

Histologically, most severe joint lesions were observed in the IPA i.v. group with a predominantly chronic inflammatory type (lymphoplasmahistiocytic cell infiltrates and granulation tissue). Chlamydiae are able to persist in their host triggering ongoing inflammatory responses resulting in chronicity.<sup>5</sup> The intravenously inoculated E58 strain resulted in mild histological joint lesions while the same strain inoculated intraarticularly resulted in severe lesions. For the IPA strain, both inoculation routes resulted in moderate to severe lesions. Altogether, the results suggest that the IPA isolate is more virulent than E58 in this challenge model. Previous potential explanations for this difference<sup>22</sup> include that, (i) the IPA strain was originally isolated from a sheep with polyarthritis and is better adapted to this host (ii) the conversion of reticulate to elementary bodies *in vitro* is six hours earlier in IPA than E58 possibly resulting in more replication competence<sup>21</sup>, and (iii) previous studies demonstrated pathogenetic diversity caused by minor genomic variations among different *Chlamydia* strains.<sup>39,27</sup> Moreover, previous *in vivo* and *in vitro* investigations<sup>21,25</sup> indicated that the *C. pecorum* IPA isolate is a plasmid-bearing strain while E58 is not and a direct relationship between the presence of a plasmid and the strain

virulence is strongly suspected. Chlamydial release via host cell lysis appears to be plasmid regulated<sup>53</sup> and results in more infectious EBs available to infect the neighbouring cells.

In naturally infected sheep (n=5), the majority of joint lesions were chronic-active inflammatory lesions (lymphoplasmahistiocytic and purulent arthritis/synovitis) (4/5 animals), while the majority of joints of experimentally infected animals showed chronic inflammatory lesions without active components (lymphoplasmahistiocytic including granulation tissue). Although experimentally and naturally infected animals were in the same age range, the duration of the *C. pecorum* infection in naturally infected animals is unknown preventing a direct comparison.

Immunohistochemistry (IHC) detected chlamydial antigen in the carpal joint of animal 628 from the IPA i.a. group, in the stifle joint of animal 658 from the IPA i.v. group and in carpal, hock and stifle joint of animal 710 from E58 i.a. group. Chlamydial inclusions were found in macrophages and occasional in synovial fibroblasts and synoviocytes. Similar to these investigations, other studies described epithelial or epithelial-like cells as primary chlamydial host cells.<sup>12</sup> Also synoviocytes have been found to be suitable host cells for *C. trachomatis*<sup>20</sup> and *C. pecorum* isolates can infect circulating monocytes/macrophages.<sup>21,14</sup> This, and the detection of *C. pecorum* DNA in blood and organs, the detection of IgG and IgM antibodies in sera of infected animals and the isolation of live organisms from joints of i.v. infected animals as described<sup>22</sup> leads to the assumption, that there is systemic, hematogenous spreading of *C. pecorum*, possibly with the help of macrophages.

Chlamydial antigen was rarely detected by IHC in joint tissues and tissues of inner organs of experimentally infected animals, whereas the corresponding qPCRs were positive in joints (53.44%) and inner organs (40.83%). In naturally infected animals,

chlamydial antigen was detected in 5/5 animals by IHC in joint tissues and tissues of inner organs, whereas the corresponding qPCRs were positive in 4/5 joint tissues from three animals. A low amount of antigen, visible in only single positive cells could indicate a low level or subclinical infection which could explain the low levels of IHC positivity.<sup>9</sup> Furthermore, IHC only detects inclusions while PCR also detects individual elementary and reticulate bodies as well as providing an estimate of DNA copies and is therefore the more sensitive method. Moreover, sections taken from various levels of a FFPE block are unable to be compared directly with PCR and IHC investigations.<sup>6</sup>

In this study, chlamydial IHC results have been included in our newly developed semi-quantitative scoring system for the assessment of histomorphological joint lesions. The first step towards the development of our scoring system was the identification of previously established scoring systems.<sup>34,29,16</sup> After the designation of inflammatory features, it was important to avoid extreme ranges of severity levels<sup>42</sup> to create an adaptive, reproducible and easily applicable scoring system which started with an unblinded initial evaluation, followed by a targeted masked review.<sup>31</sup> The inflammatory features have been determined (i) on the basis of standard definitions for chronic/active inflammations under the supervision of a dipl. ECVP pathologist and (ii) based on the comparison of synovial pathology features with normal synovial tissue as previously assessed for human rheumatology research.<sup>10,15</sup> Interestingly, calculation of the mean scores of all groups revealed the highest score in stifle joints, followed by carpal and hock joints, although the administration route in the i.a. group was the carpal joint. The reasons for the stifle joint as a predilection site remains unclear but might be the result of rapid systemic spread of the infection.

To our knowledge, a thorough description of *C. pecorum*-induced histopathological lesions in inner organs of sheep has not been performed until now. Histologically, severe lesions in experimentally infected animals were observed in the kidneys, most severe in the IPA i.v. group. The kidneys showed a chronic or chronic-active pyelitis, which partially ascended into the interstitium. As seen in the IPA i.v. group, in 5/5 animals of naturally infected animals, a chronic (animals number 3619 and 7629) or chronic-active (animals number 8452, 7578 and 8084) pyelitis, which partially ascended into the interstitium, was seen. In koalas, a thorough investigation of organ distribution and histopathological findings due to chlamydial infection was performed and 6/23 koalas showed pan-glomerular sclerosis, mild glomerulonephritis and also chronic interstitial nephritis with severe chronic-active pyelitis.<sup>9</sup> Another study revealed, that genetically distinct *C. pecorum* strains have distinct tissue tropisms in the koala and that plasmid bearing *C. pecorum* strains in the upper genital tract correlates with urogenital disease, suggesting that plasmids expand the genetic diversity of the infecting *Chlamydia*, and can increase virulence.<sup>36</sup> Thus, there are similarities between kidney lesions in koalas and sheep due to an infection with *C. pecorum*.

Interestingly, 4/20 infected sheep of both groups (IPA i.a. (n=1), IPA i.v. (n=2), E58 i.v. (n=2) showed a mild chronic lymphohistiocytic (meningo-) encephalitis which have been to our knowledge only reported in calves due to *C. pecorum* and dogs due to the chlamydial agent of ovine polyarthritis, strains LW 679 and LW 38 until now.<sup>48,49,54</sup>

In experimentally infected animals, immunohistochemical labeling to detect Iba1 (macrophages), CD20 (B cells) and CD3 (T cells) antigens was histologically most obvious for detecting macrophages, followed by B cells and T cells with the highest



presence in carpal joints followed by stifle and hock joints. In naturally infected animals, immunohistochemical labeling to detect macrophages, B and T cells, was also most obvious for detecting macrophages. Macrophages as well as monocytes and mucosal epithelial cells of respiratory, gastrointestinal, urogenital tract or conjunctival epithelium as well as trophoblastic epithelium of the placenta are well known as chlamydial target cells.<sup>44,32,38</sup> In human medicine, previous observations indicated, that monocytic cells constitute the primary host cell type for *C. trachomatis*-induced reactive arthritis in synovial tissue.<sup>11</sup> Former research groups detected *C. trachomatis* inclusions within blood monocytes via transmission electron microscopy and chlamydial major outer membrane protein via immunoelectron microscopy.<sup>30</sup>

## Conclusions

The objective of the present study was to investigate histologic changes due to *C. pecorum* in tissues of carpal, hock and stifle joints as well as spleen, liver, kidney, lymph nodes and brain of 35 sheep. The most obvious inflammatory lesions were observed in joints and the renal pelvis from experimentally, especially in the IPA-infected group, and naturally infected animals. The immunohistochemical assessment of presence and distribution of macrophages, T and B cells in joints revealed the highest presence of macrophages. Former observations, that *C. pecorum* infected circulating monocytes and our findings of histological lesions in joints and inner organs with the detection of *C. pecorum* DNA, underlines the assumption of a systemic, hematogenous spread of this agent. In human medicine, monocytic cells constitute the primary host cell type for *C. trachomatis*-induced reactive arthritis in synovial tissue. The immunohistochemical assessment, reported

here, with the highest presence of macrophages has led to the assumption that monocytic cells also constitute the primary host cell type for *C. pecorum*. This is a valuable finding for further investigations regarding the pathogenesis of *C. pecorum* and the development of a vaccine in order to minimize the consequences of chlamydial polyarthritis and the economic losses due to *C. pecorum* infection.

## **Acknowledgements**

The authors wish to thank all collaborators from the University of the Sunshine Coast, Australia. We thank the laboratory of the Institute of Veterinary Pathology, Vetsuisse Faculty, University of Zurich, Switzerland, for preparing the FFPE blocks, histological and immunohistochemical sections (Theresa Pesch, Sabina Wunderlin, Barbara Prähauser). We acknowledge the NSW DPI, Elizabeth Macarthur Agricultural Institute, where the experimental infection trial was conducted. Many thanks to Mark Hazelton, Sam Gilchrist, Ronald Coilparampil, Leah Stroud, Shayne Fell, Greg Glasgow and Kim Koeford. We thank the owners and staff from the farm in Western Australia for their assistance in providing access to their sheep and facilities for this study, and ongoing support for research into sheep health, welfare and production. We would like to thank Jeanne Peter from Vetcom, Vetsuisse Faculty, University of Zurich, Switzerland for her help in designing the figure plates.

## **Declaration of Conflicting Interests**

The authors declared no potential conflicts of interest with respect to the research, authorship, and/or publication of this article.

## Funding

Meat and Livestock Australia and the Australian Wool Innovation supported Science and Innovation Award for Young People in Agriculture, Fisheries and Forestry provided funding to projects for which naturally infected sheep were identified and samples were provided for this study.

## References

1. Bachmann NL, Frauser AT, Bertelli C, et al. Comparative genomics of koala, cattle and sheep strains of *Chlamydia pecorum*. *BMC Genomics*. 2014;15(1):667.
2. Bates D, Maechler M, Bolker B, et al. Fitting Linear Mixed-Effects Models Using lme4. *J Stat Softw*. 2015;67(1):1-48.
3. Boes KM, Durham AC. Bone Marrow, Blood Cells, and the Lymphoid/ Lymphatic System. In: Zachary JF, ed. *Pathologic Basis of Veterinary Disease* 6 th ed. St. Louis, Missouri: Elsevier; 2017:776-777.
4. Bommana S, Walker E, Desclozeaux M, et al. Humoral immune response against two surface antigens of *Chlamydia pecorum* in vaccinated and naturally infected sheep. *PloS One*. 2017;12(11):0188370.

5. Borel N, Pospischil A, Hudson AP, et al. The role of viable but non-infectious developmental forms in chlamydial biology. *Front Cell Infect Microbiol.* 2014; 4:97.
6. Borel N, Marti H, Pospischil A, et al. Chlamydiae in human intestinal biopsy samples. *Pathog Dis.* 2018; 76(8):fty081.
7. Borel N, Polkinghorne A, Pospischil A. A Review on Chlamydial Diseases in Animals: Still a Challenge for Pathologists? *Vet Pathol.* 2018;55(3):374-390.
8. Brooks ME, Kristensen K, van Benthem KJ, et al. M. glmmTMB Balances Speed and Flexibility Among Packages for Zero-inflated Generalized Linear Mixed Modeling. *The R Journal.* 2017;9(2):378-400.
9. Burach F, Pospischil A, Hanger J, et al. *Chlamydiaceae* and *Chlamydia*-like organisms in the koala (*Phascolarctos cinereus*) organ distribution and histopathological findings. *Vet Microbiol.* 2014;172:230-240.
10. Cake MA, Smith MM, Young AA, et al. Synovial pathology in an ovine model of osteoarthritis: effect of intraarticular hyaluron (Hyalgan). *Clin Exp Rheumatol.* 2008;26:561-587.
11. Carter JD, Gerard HC, Whittum-Hudson JA, et al. Combination antibiotics for the treatment of *Chlamydia*-induced reactive arthritis: is a cure in sight? *Int J Clin Rheumatol.* 2011;6(3):333-345.

- 641
- 642 12. Carter JD, Gerard HC, Whittum-Hudson JA, et al. The molecular basis for
- 643 disease phenotype in chronic Chlamydia-induced arthritis. *Int J Clin*
- 644 *Rheumatol.* 2012;7(6):627-640.
- 645
- 646 13. Clarkson MJ, Philips HL. Isolation of faecal chlamydia from sheep in Britain
- 647 and their characterization by cultural properties. *Vet J.* 1997;153(3):307-310.
- 648
- 649 14. Ersdal C, Jørgensen HJ, Lie K-I. Acute and Chronic *Erysipelothrix*
- 650 *rhusiopathiae* Infection in Lambs. *Vet Pathol.* 2015;52(4):635-643.
- 651
- 652 15. Fumitomo K, Hiroaki M, Kunihiro W, et al. Synovitis in rheumatoid arthritis:
- 653 Scoring of characteristic histopathological features. *Pathol Int.* 1999;49:298-
- 654 304.
- 655
- 656 16. Gibson-Corley KN, Olivier AK, Meyerholz DK. Principles for valid
- 657 histopathologic scoring in research. *Vet Pathol.* 2013;50(6):1007-1015.
- 658
- 659 17. Griffith JE, Dhand NK, Krockenberger MB, et al. A retrospective study of
- 660 admission trends of koalas to a rehabilitation facility over 30 years. *J Wildl*
- 661 *Dis.* 2013;49:18–28.
- 662
- 663 18. Hothorn T, Bretz F, Westfall P. Simultaneous Inference in General Parametric
- 664 Models. *Biom J.* 2008;50(3):346-363.

- 665
- 666 19. Højsgaard S, Halekoh U, Yan J. The R Package geepack for Generalized Esti  
667 mating Equations Journal of Statistical Software. 2006;15(2):1-11.
- 668
- 669 20. Inman RD, Chiu B. Synoviocyte-Packaged *Chlamydia trachomatis* Induces a  
670 Chronic Aseptic Arthritis. *J Clin Invest.* 1998;102(10):1776–1782.
- 671
- 672 21. Islam MM, Jelocnik M, Anstey S, et al. *In Vitro* Analysis of Genetically Distinct  
673 *Chlamydia Pecorum* Isolates Reveals Key Growth Differences in Mammalian  
674 Epithelial and Immune Cells. *Vet Mic.* 2019; 232:22-29.
- 675
- 676 22. Islam MM. Understanding the pathogenesis of *Chlamydia pecorum* infections  
677 in livestock. 2019. PhD thesis. University of the Sunshine Coast, Sippy  
678 Downs, Australia.
- 679
- 680 23. Jelocnik M, Frentiu FD, Timms P, et al. Multilocus sequence analysis provides  
681 insights into molecular epidemiology of *Chlamydia pecorum* infections in  
682 Australian sheep, cattle, and koalas. *J Clin Microbiol.* 2013;51(8):2625-2632.
- 683

24. Jelocnik M, Forshaw D, Cotter J, et al. Molecular and pathological insights into *Chlamydia pecorum*-associated sporadic bovine encephalomyelitis (SBE) in Western Australia. *BMC Vet Res.* 2014;10:121.

25. Jelocnik M, Bachmann NL, Kaltenboeck B, et al. Genetic diversity in the plasticity zone and the presence of the chlamydial plasmid differentiates *Chlamydia pecorum* strains from pigs, sheep, cattle, and koalas. *BMC Genomics.* 2015;16:893.

26. Jelocnik M, Islam MM, Madden D, et al. Development and evaluation of rapid novel isothermal amplification assays for important veterinary pathogens: *Chlamydia psittaci* and *Chlamydia pecorum*. *PeerJ.* 2017;5:3799.

27. Kari L, Whitmire WM, Carlson JH, et al. Pathogenic diversity among *Chlamydia trachomatis* ocular strains in nonhuman primates is affected by subtle genomic variations. *J Infect Dis Lett.* 2008;197(3):449-456.

28. Koizumi F, Matsuno H, Wakaki K, et al. Synovitis in rheumatoid arthritis: Scoring of characteristic histopathological features. *Pathol Int.* 1999;49:298-304.

29. Klopfleisch R. Multiparametric and semiquantitative scoring systems for the evaluation of mouse model histopathology- a systemic review. *BMC Vet Res.* 2013;9:123.
30. Köhler L, Nettelbreker E, Hudson AP. Ultrastructural and molecular analysis of the persistence of *Chlamydia trachomatis* (serovar K) in human monocytes. *Microb Pathogen.* 1997;22:133–142.
31. La Perle K. Comparative Pathologists: Ultimate Control Freaks seeking validation! *Vet Pathol.* 2019;56(1):19-23.
32. Longbottom D, Coulter L.J. Animal Chlamydioses and zoonotic implications. *J Comp Path.* 2003;128:217–244.
33. McNutt S, Waller EF. Sporadic bovine encephalomyelitis (Buss disease). *Cornell Vet.* 1940;30:437-448.
34. Meyerholz DK, Beck A. Principles and approaches for reproducible scoring of tissue stains in research. *Lab Invest.* 2018;98:844-855.
35. Page LC. Chlamydial polyarthritis in Iowa lambs. *Iowa State Univ Vet.* 1968; 39:10-18.



36. Phillips S, Robbins A, Loader J, et al. *Chlamydia pecorum* gastrointestinal tract infection associations with urogenital tract infections in the koala (*Phascolarctos cinereus*). *PLoS One*. 2018;13:12.
37. Polkinghorne A, Hanger J, Timms P. Recent advances in understanding the biology, epidemiology and control of chlamydial infections in koalas. *Vet Microbiol*. 2013;165(3-4):214-223.
38. Pospischil A, Borel N, Andersen AA. *Chlamydia*. In: Gyles, C., Prescott, J., Songer, G. (Eds.), *Pathogenesis of Bacterial Infections in Animals*. 4th ed. Wiley-Blackwell, Hoboken, NJ, 2010;575–588.
39. Ramsey KH, Sigar IM, Schripsema JH, et al. Strain and virulence diversity in the mouse pathogen *Chlamydia muridarum*. *Infect Immun*. 2009;77(8):3284-3293.
40. R core team (2020). A language and environment for statistical computing. R Foundation for Statistical Computing, Vienna, Austria. URL <https://www.R-project.org/>.
41. Sait M, Livingstone M, Clark EM, et al. Genome sequencing and comparative analysis of three *Chlamydia pecorum* strains associated with different pathogenic outcomes. *BMC Genomics*. 2014;15:23.

- 751
- 752 42. Schafer KA, Eighmy J, Fikes JD, et al. Use of Severity Grades to Characterize
- 753 Histopathologic Changes. *Toxicol Pathol.* 2018;46(3):256-265.
- 754
- 755 43. Schautteet K, Stuyven E, Beeckman DS, et al. Protection of pigs against
- 756 *Chlamydia trachomatis* challenge by administration of a MOMP-based DNA
- 757 vaccine in the vaginal mucosa. *Vet Res.* 2011;42:29.
- 758
- 759 44. Shewen PE. Chlamydial Infection in animals. A Review. *Can Vet J.*
- 760 1980;21:2-11.
- 761
- 762 45. Signorell A et al. (2020). DescTools: Tools for descriptive statistics. R packag
- 763 e version 0.99.34.
- 764
- 765 46. Storz J, Walter LN. Polyarthritis of lambs induced experimentally by a
- 766 psittacosis agent. *Am J Agric Res.* 1964; 115:9-18.
- 767
- 768 47. Storz J, Walter LN. Observations on Sheep with Polyarthritis Produced by an
- 769 Agent of the Psittacosis- lymphogranuloma Venerum- trachoma Group.
- 770 *Arthritis Rheumatol.* 1967;10:1.
- 771

48. Storz J, Eugster AK. Pathogenetic events in intestinal chlamydial infections leading to polyarthritis in calves. *J Infect.* 1971;123(1).
49. Storz J, Eugster AK, Altera KP, et al. Behavior of different bovine chlamydial agents in newborn calves. *J Comp Path.* 1971;81.
50. Walker E, Lee EJ, Timms P, et al. *Chlamydia pecorum* infections in sheep and cattle: A common and under-recognised infectious disease with significant impact on animal health. *Vet J.* 2015;206(3):252-260.
51. Walker E, Moore C, Shearer P, et al. Clinical, diagnostic and pathologic features of presumptive cases of *Chlamydia pecorum*-associated arthritis in Australian sheep flocks. *BMC Vet Res.* 2016;12(1):193.
52. Wilson DP, Craig AP, Hanger J, et al. The Paradox of Euthanizing Koalas (*Phascolarctos Cinereus*) to Save Populations from Elimination. *J Wildl Dis.* 2015;51(4):833–842.
53. Yang R, Jacobson C, Gardner G, et al. Corrigendum to «Longitudinal prevalence and faecal shedding of *Chlamydia pecorum* in sheep». *Vet J.* 2014;201:322-326.
54. Young S, Storz J, Maierhofer CA. Pathologic features of experimentally induced chlamydial infection in dogs. *Am J Vet Res.* 1972;33:2.

## Figure legends

**Figure 1.** Qualitative assessment of histological joint lesions. Assessment of the presence of inflammation, the type of inflammation, the degree and distribution of inflammation and whether the surrounding tissue is affected or not.

**Figure 2.** Qualitative assessment of histological lesions of inner organs. Identification of four main microscopic findings, focussing on inflammation and the qualitative assessment of the presence of inflammation, the type, degree and distribution of inflammation.

**Figure 3-10.** Histologic findings and additional synovial findings in joints of experimentally and naturally *C. pecorum* infected sheep. Hematoxylin and eosin (HE). **Figure 3.** Chronic arthritis. Carpal joint, experimentally infected animal number 328, E58 i.a. group. 100x. HE. Insert: moderate chronic multifocal lymphoplasmahistiocytic arthritis, lymphocytes (arrow) plasma cells (arrow), histiocytes (arrow). 400x. HE. **Figure 4.** Chronic arthritis with granulation tissue. Carpal joint, experimentally infected animal number 723, IPA i.a. group. Moderate chronic multifocal lymphoplasmahistiocytic arthritis with granulation tissue (arrows). 100x. HE. **Figure 5.** Chronic-active arthritis. Carpal joint, experimentally infected animal number 673, carpus, E58 i.a. group. 100x. HE. Severe chronic-active multifocal lymphohistiocytic and purulent arthritis and synovitis with fibrin accumulations (arrow). Insert: neutrophils (arrow) and fibrin (arrow). 400x. HE. **Figure 6.** Chronic-active arthritis with fibrin accumulations. Carpal joint, experimentally infected animal number 710, E58 i.a. group. 100x. HE. Severe

chronic-active multifocal lymphohistiocytic arthritis with fibrin accumulations (arrows).

Insert: plasma cells (arrow), histiocytes (arrow) and neutrophils (arrow). 400x. HE.

**Figure 7.** Additional synovial findings. Carpal joint, experimentally infected animal

number 628, IPA i.a. group. Areolar folding (arrows). 100x. HE. **Figure 8.** Additional

synovial findings. Stifle joint, experimentally infected animal number 694, E58 i.v.

group. Neovascularization (arrows) with areolar folding convoluted into

vascularised villi. 100x. HE. **Figure 9.** Active arthritis. Stifle joint, naturally infected

animal number 3619. 100x. HE. Mild to moderate active multifocal purulent synovitis.

Insert: neutrophils (arrows). 400x. HE. **Figure 10.** Chronic arthritis. Carpal joint,

naturally infected animal number 8452. 100x. HE. Moderate to severe chronic

multifocal plasmacellular arthritis. Insert: plasma cells (arrows). 400x. HE.

**Figure 11-18.** Histologic findings in inner organs of experimentally and naturally *C.*

*pecorum* infected sheep. Hematoxylin and eosin (HE). **Figure 11.** Chronic

meningoencephalitis. Brain, experimentally infected animal number 658, IPA i.v.

group. Moderate chronic multifocal lymphohistiocytic meningoencephalitis (arrows).

100x. HE. Insert: focal glia nodule. 400x. HE. **Figure 12.** BALT hyperplasia. Lung,

experimentally infected animal number 616, IPA i.v. group. 100x. HE. **Figure 13.**

Secondary follicles. Lymph node, experimentally infected animal number 710, E58

i.a. group. 100x. HE. **Figure 14.** Chronic periportal hepatitis. Liver, experimentally

infected animal number 591, E58 i.v. group. Mild to moderate chronic

lymphoplasmacellular periportal hepatitis. 100x. HE. Insert: leukocytostasis (arrows).

400x. HE. **Figure 15.** Chronic-active pyelitis. Kidney, experimentally infected animal

number 531, E58 i.v. group. Severe chronic-active multifocal purulent and

lymphohistiocytic pyelitis (arrows), ascending into the papilla. 100x. HE. Insert:

lymphocytes (arrow), macrophages (arrow), neutrophil (arrow). 400x. HE. **Figure 16.**

Chronic-active pyelitis. Kidney, experimentally infected animal number 616, IPA i.v. group. Severe chronic-active multifocal purulent and lymphoplasmahistiocytic pyelitis with follicle formation (arrows). 100x. HE. **Figure 17.** Chronic pyelitis. Kidney, naturally infected animal number 3619. Moderate to severe chronic multifocal lymphoplasmahistiocytic pyelitis. 100x. HE. Insert: lymphocytes (arrow), plasma cells (arrow), macrophages (arrow). 400x. HE. **Figure 18.** Chronic-active conjunctivitis. Conjunctiva, naturally infected animal number 3619. Severe chronic-active multifocal lymphoplasmacellular and purulent conjunctivitis with follicle formation (arrow). 100x. HE. Insert: plasma cells (arrow), neutrophils (arrow). 400x. HE.

**Figure 19-22.** Immunohistochemistry for chlamydial labeling (Chlc) in joints and inner organs of experimentally and naturally *C. pecorum* infected sheep. **Figure 19.**

Positive immunohistochemical labeling for chlamydial antigen (Chlc). Carpal joint, experimentally infected animal number 628, IPA i.a. group. 200x. Chlc. Insert: positive granular intracytoplasmic labeling, mostly in macrophages (arrows). 400x.

Chlc. **Figure 20.** Positive immunohistochemical labeling for chlamydial antigen (Chlc). Kidney, experimentally infected animal number 616, IPA i.v. group. 200x.

Chlc. Insert: positive granular intracytoplasmic labeling in the lining epithelium of the renal papilla (arrow). 400x. Chlc. **Figure 21.** Positive immunohistochemical labeling

for chlamydial antigen (Chlc). Carpal joint, naturally infected animal number 3619. 200x. Chlc. Insert: positive granular intracytoplasmic labeling, mostly in macrophages (arrows). 400x. Chlc. **Figure 22.** Positive immunohistochemical labeling for

chlamydial antigen (Chlc). Kidney, naturally infected animal number 7578. 200x. Chlc. Insert: single positive cell underneath the epithelium of the renal papilla (arrow). 400x. Chlc.

**Figure 23-28.** Immunohistochemistry for detecting macrophages (Iba1), B cells (CD20) and T cells (CD3) in joints of experimentally and naturally *C. pecorum*

infected sheep. **Figure 23.** Immunohistochemistry for detecting macrophages (Iba1). Carpal joint, experimentally infected animal number 723, IPA i.a. group. 100x. Iba1. Insert: positive immunohistochemical labeling for detecting Iba 1 antigen. 400x. Iba1.

**Figure 24.** Immunohistochemistry for detecting B cells (CD20). Carpal joint, experimentally infected animal number 628, IPA i.a. group. 100x. CD20. Insert: positive immunohistochemical labeling for detecting CD20 antigen. 400x. CD20.

**Figure 25.** Immunohistochemistry for detecting T cells (CD3). Carpal joint, experimentally infected animal number 673, E58 i.a. group. 100x. CD3. Insert: positive immunohistochemical labeling for detecting CD3 antigen. 400x. CD3. **Figure**

**26.** Immunohistochemistry for detecting macrophages (Iba1). Carpal joint, naturally infected animal number 7578. 200x. Iba1. Insert: positive immunohistochemical labeling for detecting Iba 1 antigen. 400x. Iba1. **Figure 27.** Immunohistochemistry for detecting B cells (CD20). Carpal joint, naturally infected animal number 7629. 200x. CD20. Insert: positive immunohistochemical labeling for detecting CD20 antigen.

400x. CD20. **Figure 28.** Immunohistochemistry for detecting T cells (CD3). Carpal joint, experimentally infected animal number 8452. 200x. CD3. Insert: positive immunohistochemical labeling for detecting CD3 antigen. 400x. CD3.

**Figure 29.** Mosaicplot, CD3 labeling, experimentally infected animals. The groups IPA i.a., IPA i.v. and E58 i.a. differed significantly from the control group with the highest presence in carpal joints followed by stifle and hock joints (evaluated using mixed models).

**Figure 30.** Mosaicplot, CD20 labeling, experimentally infected animals. CD20 labeling revealed a significant difference in the E58 i.a., IPA i.a. and IPA i.v. group when compared to the control group and with the highest presence in carpal joints followed by stifle and hock joints (evaluated using mixed models).

**Figure 31.** Mosaicplot, Iba1 labeling, experimentally infected animals. For Iba1 labeling, the groups E58 i.a., IPA i.v. and IPA i.a. group differed significantly from the control group with the highest presence in carpal joints followed by stifle and hock joints (evaluated using mixed models).



## Annexes

**Table 1: Euthanasia was performed at various time points after the administration of group-specific inoculum.**

group	animal ID	days after inoculation until euthanasia
control	356	22
	373	22
	351	22
	655	22
	687	15
UV i.v. <sup>a</sup>	393	15
	681	21
	685	18
	671	21
	604	21
UV i.a. <sup>b</sup>	396	21
	568	18
	595	21
	394	21
	544	15
IPA i.v. <sup>c</sup>	335	21
	658	15
	320	9
	591	21
	616	18
IPA i.a. <sup>d</sup>	628	21
	661	10
	578	10
	723	9
	716	18
E 58 i.v. <sup>e</sup>	365	21
	694	15

	593	18
	339	4
	531	21
E58 i.a. <sup>f</sup>	370	15
	328	18
	710	9
	315	4
	673	21

<sup>a</sup>*C. pecorum*, UV- irradiated. Route of administration: intravenous (i.v.)

<sup>b</sup>*C.pecorum*, UV- irradiated. Route of administration: intraarticular (i.a.)

<sup>c</sup>*C. pecorum*, strain IPA. Route of administration: intravenous (i.v.)

<sup>d</sup>*C. pecorum*, strain IPA. Route of administration: intraarticular (i.a.)

<sup>e</sup>*C. pecorum*, strain E58. Route of administration: intravenous (i.v.)

<sup>f</sup>*C. pecorum*, strain E58. Route of administration: intraarticular (i.a.)

**Table 2: Semiquantitative parameters (scoring system) for the histological examination of joint lesions.**

para- meters	score	0	1	2	3	maximal score per joint	maximal score per animal
inflammation	numbers of foci per section	0	1-5	6-10	>10	3	9
	distribution						
	acute		focal	multifocal	diffuse		
	degree	npf <sup>a</sup>	mild <sup>b</sup>	moderate <sup>c</sup>	severe <sup>d</sup>	3	9
	numbers of foci per section	0	1-5	6-10	>10	3	9
	distribution						
	chronic		focal	multifocal	diffuse		
	degree	npf <sup>a</sup>	mild <sup>b</sup>	moderate <sup>c</sup>	severe <sup>d</sup>	3	9
	presence of fibrin	no	yes	n/a <sup>e</sup>	n/a <sup>e</sup>	1	3
	presence of granulation tissue	no	yes	n/a <sup>e</sup>	n/a <sup>e</sup>	1	3

<b>surrounding tissue affected</b>	no	yes	n/a <sup>e</sup>	n/a <sup>e</sup>	1	3
<b>IHC positive</b>	no	yes	n/a <sup>e</sup>	n/a <sup>e</sup>	1	3
<b>maximal total score</b>					<b>16</b>	<b>48</b>

<sup>a</sup>npf = no pathological findings

<sup>b</sup>mild = low number of inflammatory cells

<sup>c</sup>moderate = moderate number of inflammatory cells

<sup>d</sup>severe = severe number of inflammatory cells

<sup>e</sup>n/a= analysis was not applicable

**Table 3: Additional histological findings in joints of experimentally infected animals.**

	animal/ group						
	control	UV, i.a. <sup>a</sup>	UV, i.v. <sup>b</sup>	E58, i.a. <sup>c</sup>	E58, i.v. <sup>d</sup>	IPA, i.a. <sup>e</sup>	IPA, i.v. <sup>f</sup>
<b>synoviocyte proliferation</b>	0/5	1/5	0/5	5/5	4/5	5/5	5/5
- palisading							
- areolar folding							
<b>neovascularisation</b>	0/5	0/5	0/5	4/5	2/5	3/5	5/5
- areolar folding							
convoluted into							
vascularised							
villi							
<b>periarterial fibrosis</b>	0/5	0/5	0/5	2/5	1/5	2/5	4/5
<b>total score/ group</b>	<b>0</b>	<b>1</b>	<b>0</b>	<b>11</b>	<b>7</b>	<b>10</b>	<b>14</b>

<sup>a</sup>*C. pecorum*, UV- irradiated. Route of administration: intraarticular (i.a.)

<sup>b</sup>*C. pecorum*, UV- irradiated. Route of administration: intravenous (i.v.)

<sup>c</sup>*C. pecorum*, strain E58. Route of administration: intraarticular (i.a.)

<sup>d</sup>*C. pecorum*, strain E58. Route of administration: intravenous (i.v.)

<sup>e</sup>*C. pecorum*, strain IPA. Route of administration: intraarticular (i.a.)

<sup>f</sup>*C. pecorum*, strain IPA. Route of administration: intravenous (i.v.)

**Table 4: Semiquantitative parameters (scoring system) for the histological examination of inner organs (brain, kidney, liver).**

parameters	score	0	1	2	3	maximal score per organ	maximal score per animal
acute	numbers of foci per section	0	1-5	6-10	>10	3	9
	distribution		focal	multifocal	diffuse		
	degree	npf <sup>a</sup>	mild <sup>b</sup>	moderate <sup>c</sup>	severe <sup>d</sup>	3	9
inflammation chronic	numbers of foci per section	0	1-5	6-10	>10	3	9
	distribution		focal	multifocal	diffuse		
	degree	npf <sup>a</sup>	mild <sup>b</sup>	moderate <sup>c</sup>	severe <sup>d</sup>	3	9
IHC positive	n/a <sup>e</sup>	no	yes	n/a <sup>e</sup>	n/a <sup>e</sup>	1	3
maximal total score						13	39

<sup>a</sup>npf= no pathological findings

<sup>b</sup>mild = low number of inflammatory cells

<sup>c</sup>moderate = moderate number of inflammatory cells

<sup>d</sup>severe = severe number of inflammatory cells

<sup>e</sup>n/a= analysis was not applicable

**Table 5: Antibodies used for immunophenotyping of macrophages, B- and T- lymphocytes in joints.**

	<b>primary antibody</b>	<b>epitope demasking</b>	<b>dilution</b>	<b>incubation</b>	<b>secondary antibody</b>
<b>CD3</b>	DAKO, M7254	Dkb <sup>a</sup> (pH9, 98°C, 20 min)	1:50	1h	EnV.Ms <sup>b</sup> , substrate DAB
<b>CD20</b>	Thermo Scientific, RB9013-P	without	1:100	30min	EnV.Rb <sup>c</sup> , substrate DAB
<b>Iba 1</b>	WAKO, 019- 19741	Dkc <sup>d</sup> (pH6, 98°C, 20 min)	1:350	1h	EnV.Rb <sup>c</sup> , substrate DAB

<sup>a</sup>basic buffer heat

<sup>b</sup>Envision mouse antibody

<sup>c</sup>Envision rabbit antibody

<sup>d</sup>citrat buffer heat



**Table 6: Histopathologic joint diagnoses in experimentally infected animals grouped according to inoculum, route of administration, immunohistochemistry, total semiquantitative score per group and additional findings.**

group	chronic inflammation <sup>a</sup>	chronic-active/ active inflammation <sup>b</sup>	score	Chlc <sup>c</sup>	additional findings <sup>d</sup>
control	1/15 <sup>e</sup>	0/15	6	negative	0
UV- IPA, i.a. <sup>f</sup>	2/15	1/15 <sup>g</sup>	10	negative	1
UV- IPA, i.v. <sup>h</sup>	2/15	0/15 <sup>i</sup>	8	negative	0
E58, i.a. <sup>j</sup>	5/15	7/15	74	positive (1/5)	11
E58, i.v. <sup>k</sup>	3/15	2/15	18	negative	7
IPA, i.a. <sup>l</sup>	1/15	5/15	66	positive (1/5)	10
IPA, i.v. <sup>m</sup>	8/15	5/15	79	positive (1/5)	14

<sup>a</sup>number of joints per group with chronic arthritis/ synovitis. In total: fifteen joints per group (carpal, hock and stifle joint per animal)

<sup>b</sup> number of joints per group with chronic- active or active arthritis/ synovitis. In total: fifteen joints per group (carpal, hock and stifle joint per animal)

<sup>c</sup>IHC to detect chlamydial antigen

<sup>d</sup>additional findings: score per group

<sup>e</sup>one case: acute periartthritis, possibly injection- site induced, not included in scoring

<sup>a</sup>*C. pecorum*, UV- irradiated. Route of administration: intraarticular (i.a.)

<sup>a</sup>one case: acute focal fibrositis, not included in scoring

<sup>b</sup>*C. pecorum*, UV- irradiated. Route of administration: intravenous (i.v.)

<sup>b</sup>one case: acute focal cellulitis and hemorrhage, not included in scoring

<sup>c</sup>*C. pecorum*, strain E58. Route of administration: intraarticular (i.a.)

<sup>c</sup>*C. pecorum*, strain E58. Route of administration: intravenous (i.v.)

<sup>d</sup>*C. pecorum*, strain IPA. Route of administration: intraarticular (i.a.)

<sup>d</sup>*C. pecorum*, strain IPA. Route of administration: intravenous (i.v.)

**Table 7: Histopathologic diagnoses of inner organs (brain, kidney, liver) of experimentally infected animals grouped according to inoculum, route of administration, immunohistochemistry, total semiquantitative score per group and additional findings.**

group	organ	chronic inflammation <sup>a</sup>	active inflammation <sup>b</sup>	score	Chlc <sup>c</sup>
<b>control</b>	brain	0/5 <sup>d</sup>	0/5	6	negative
	kidney	0/5	0/5		
	liver	1/5 <sup>e</sup>	1/5 <sup>f</sup>		
<b>UV- IPA, i.a.<sup>g</sup></b>	brain	1/5 <sup>h</sup>	0/5	12	negative
	kidney	0/5	0/5		
	liver	3/5	1/5 <sup>f</sup>		
<b>UV- IPA, i.v.<sup>i</sup></b>	brain	0/5 <sup>d</sup>	0/5	6	negative
	kidney	0/5	0/5		
	liver	1/5	1/5 <sup>f</sup>		
<b>E58, i.a.<sup>j</sup></b>	brain	0/5	0/5	26	negative
	kidney	3/5 <sup>k,l</sup>	1/5		
	liver	3/5	0/5		
<b>E58, i.v.<sup>m</sup></b>	brain	2/5 <sup>d</sup>	0/5	32	negative
	kidney	0/5	2/5 <sup>f</sup>		

	liver	3/5	3/5		
<b>IPA, i.a.<sup>n</sup></b>	brain	1/5	0/5	15	positive (1/5)
	kidney	2/5	0/5		
	liver	1/5	3/5		
<b>IPA, i.v.<sup>o</sup></b>	brain	2/5	0/5	60	positive (2/5)
	kidney	1/5 <sup>k</sup>	3/5 <sup>f</sup>		
	liver	1/5	3/5		

<sup>n</sup>number of inner organs per group with chronic inflammation.

<sup>n</sup>number of inner organs per group with chronic-active or active inflammation.

<sup>i</sup>Immunohistochemistry to detect Chlamydial antigen.

<sup>d</sup>1/5= mild and focal chronic encephalitis, not included in scoring.

<sup>e</sup>1/5= mild and focal chronic periportal hepatitis, not included in scoring.

<sup>f</sup>leukocytostasis.

<sup>g</sup>*C. pecorum*, UV- irradiated. Route of administration: intraarticular (i.a.).

<sup>h</sup>focal glia nodule, negative tested for toxoplasma antigen.

<sup>i</sup>*C. pecorum*, UV- irradiated. Route of administration: intravenous (i.v.).

<sup>j</sup>*C. pecorum*, strain E58. Route of administration: intraarticular (i.a.).

<sup>k</sup>also interstitial nephritis.

<sup>l</sup>1/5= mild chronic and focal lymphocytic pyelitis, not included in scoring.

<sup>m</sup>*C. pecorum*, strain E58. Route of administration: intravenous (i.v.).

<sup>n</sup>*C. pecorum*, strain IPA. Route of administration: intraarticular (i.a.).

<sup>o</sup> *C. pecorum*, strain IPA. Route of administration: intravenous (i.v.).

Figure 1:

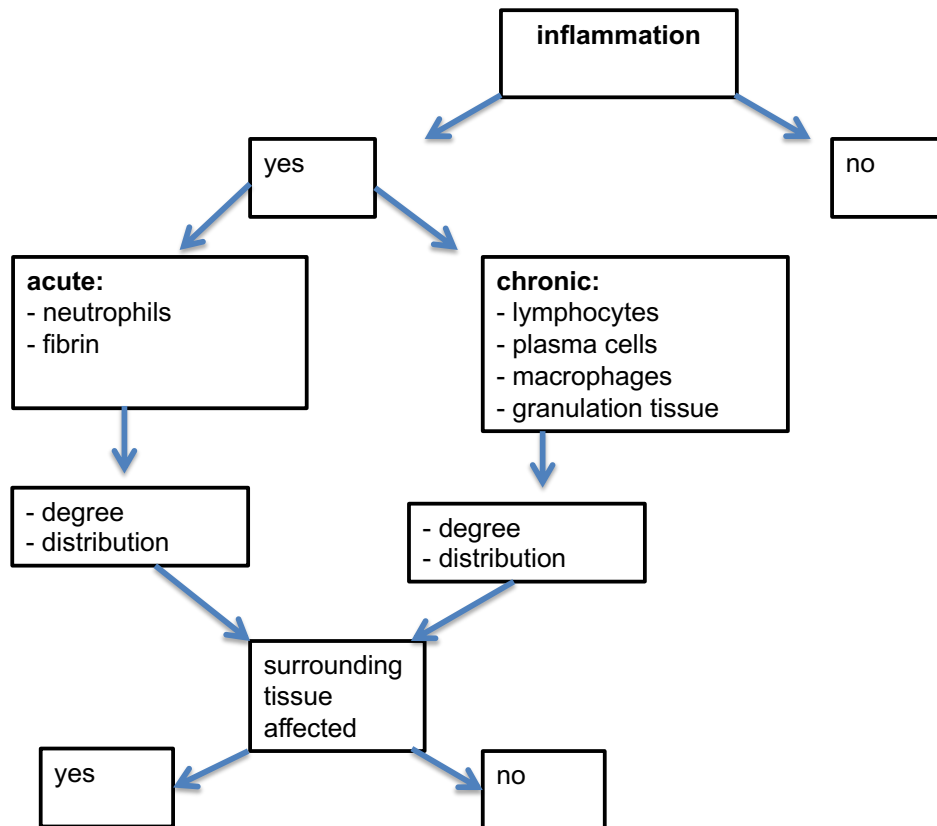


**Figure 2:**

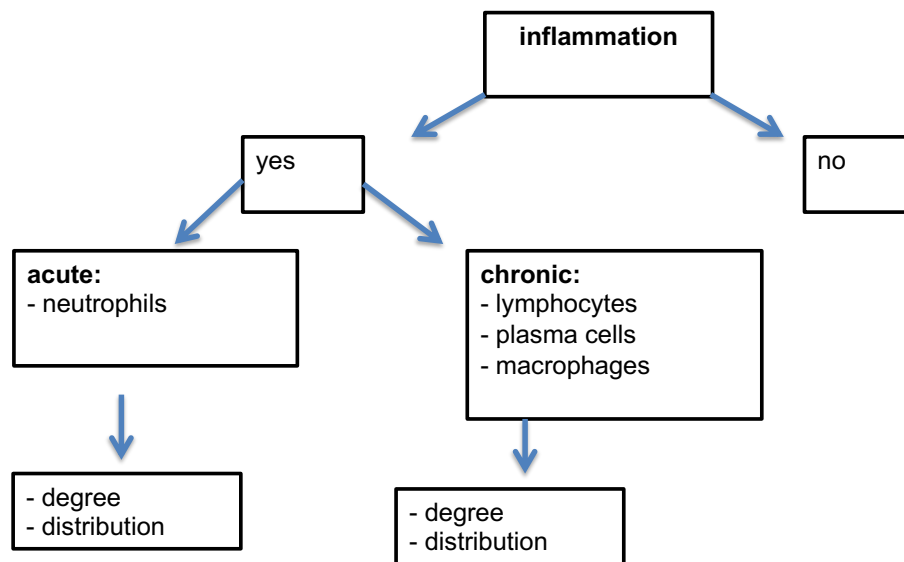


**Figure 3-10:**

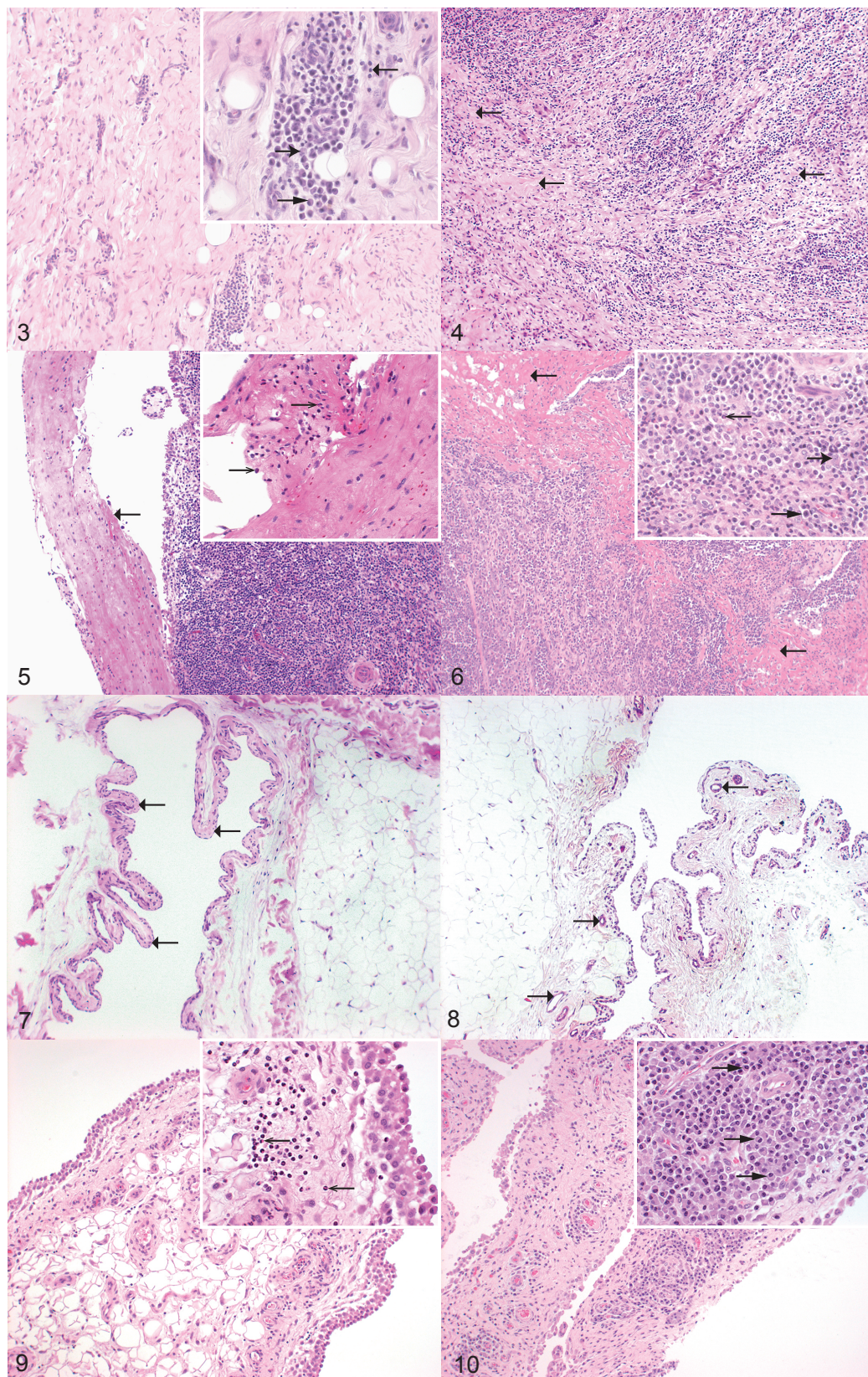




**Figure 11-18:**

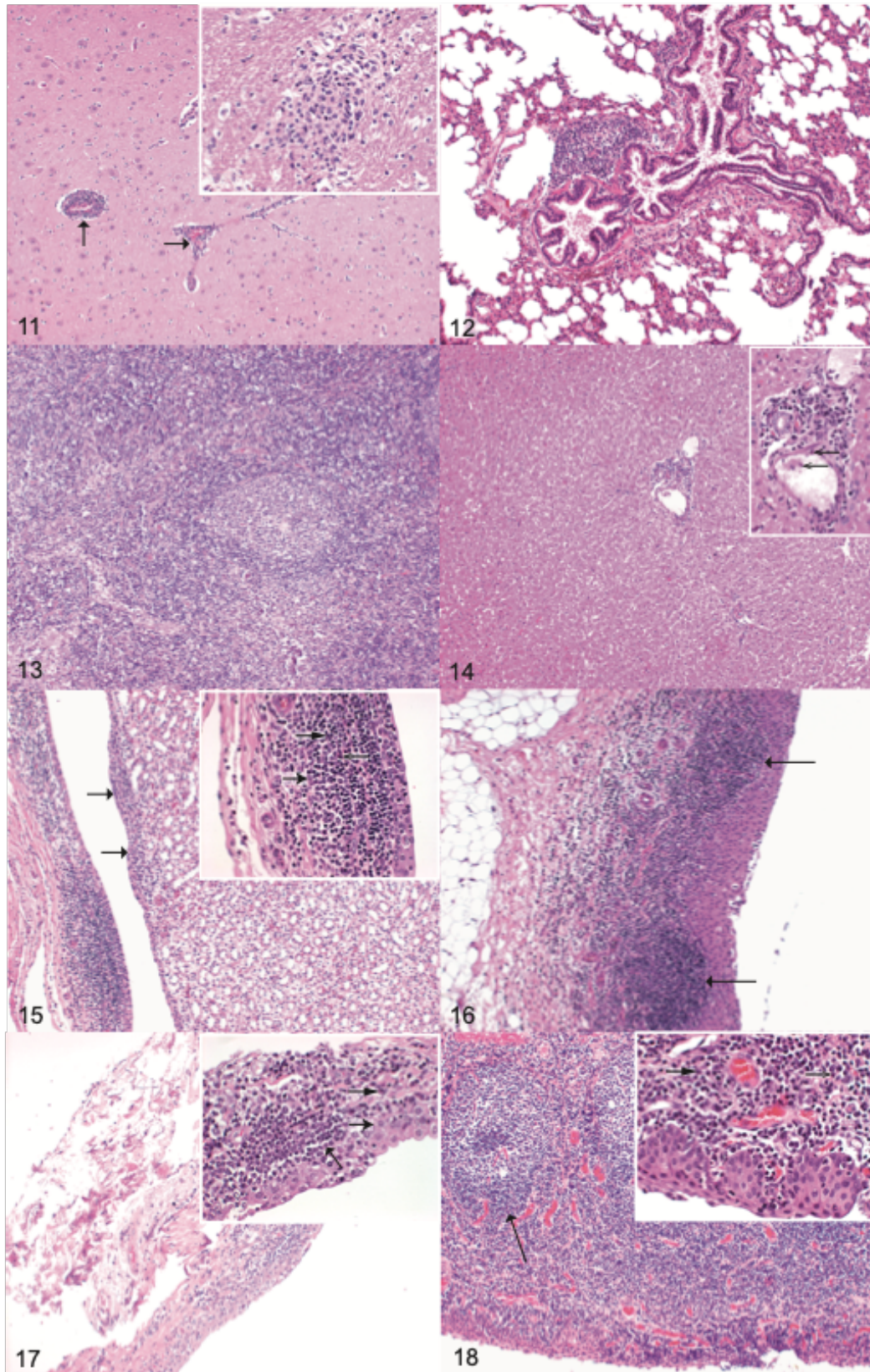




**Figure 19-22:**

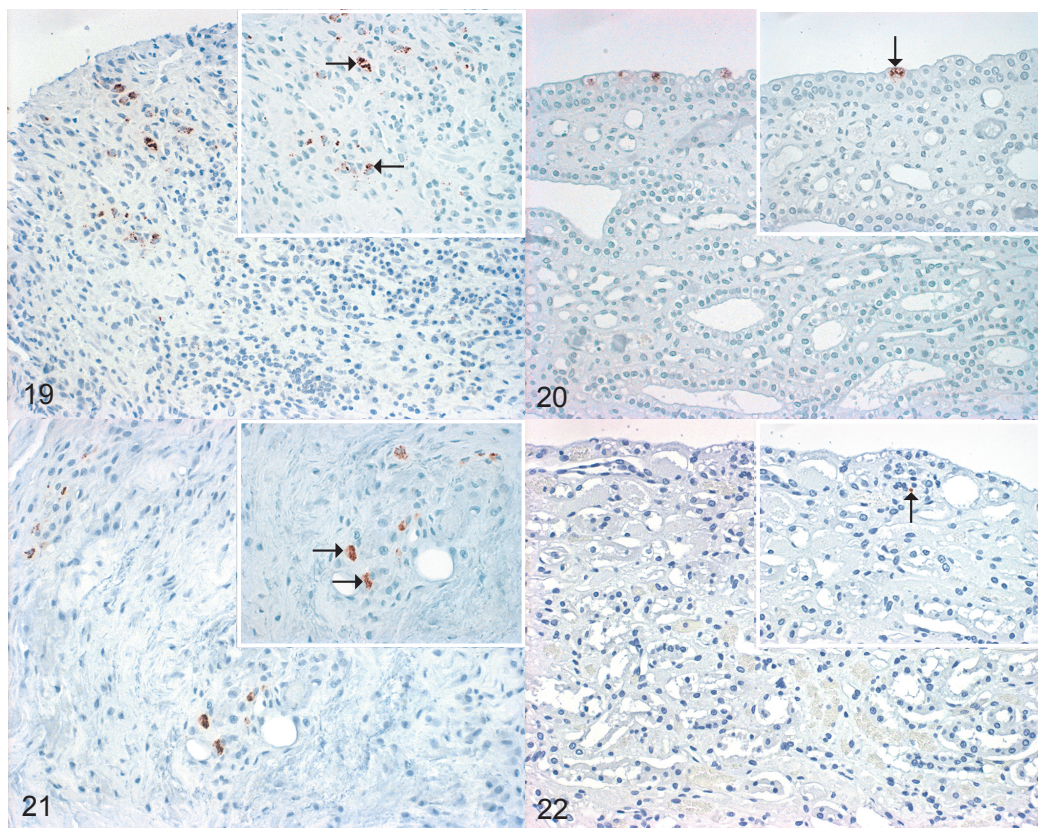




**Figure 23-28:**

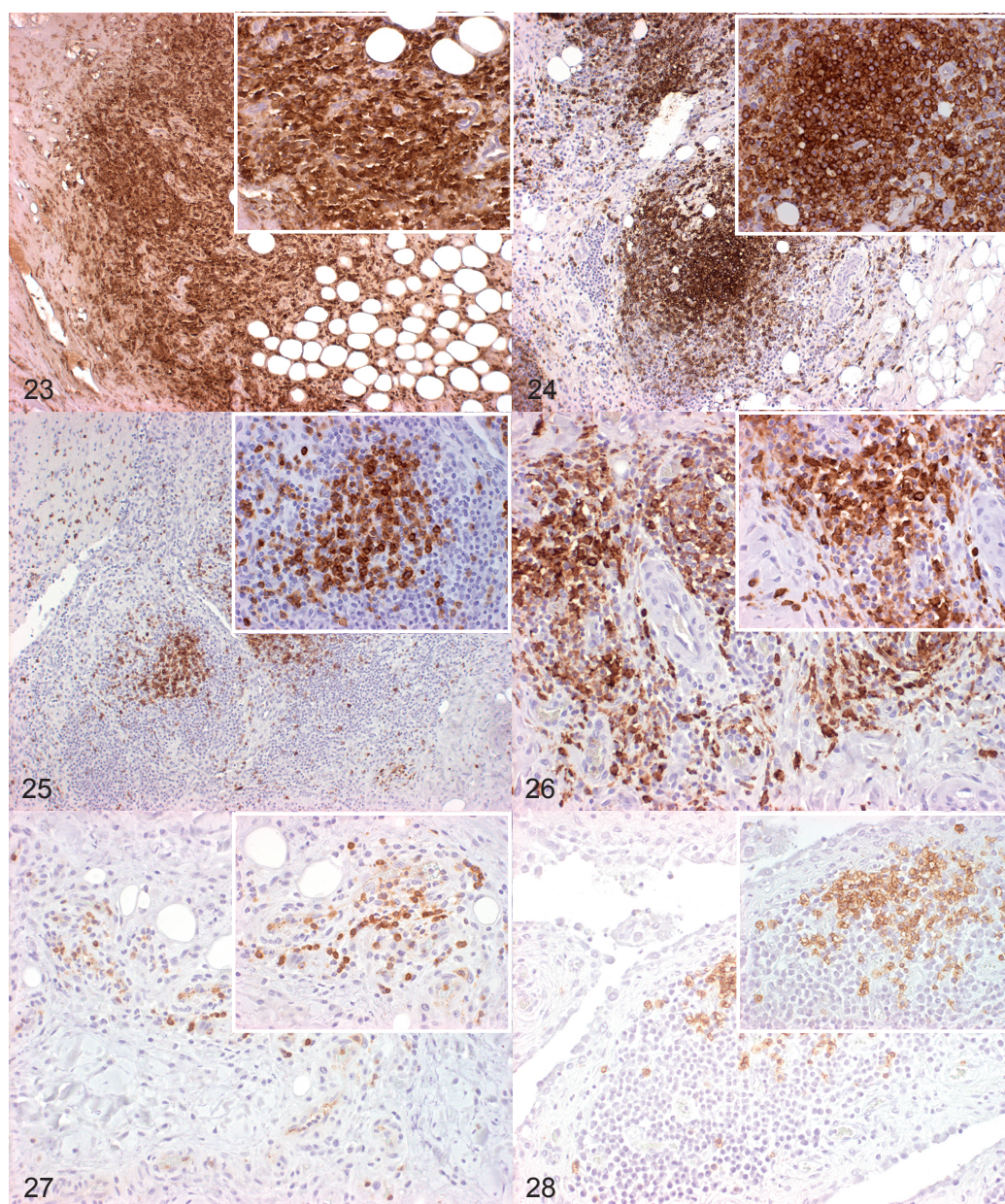


Figure 29:



Figure 30:

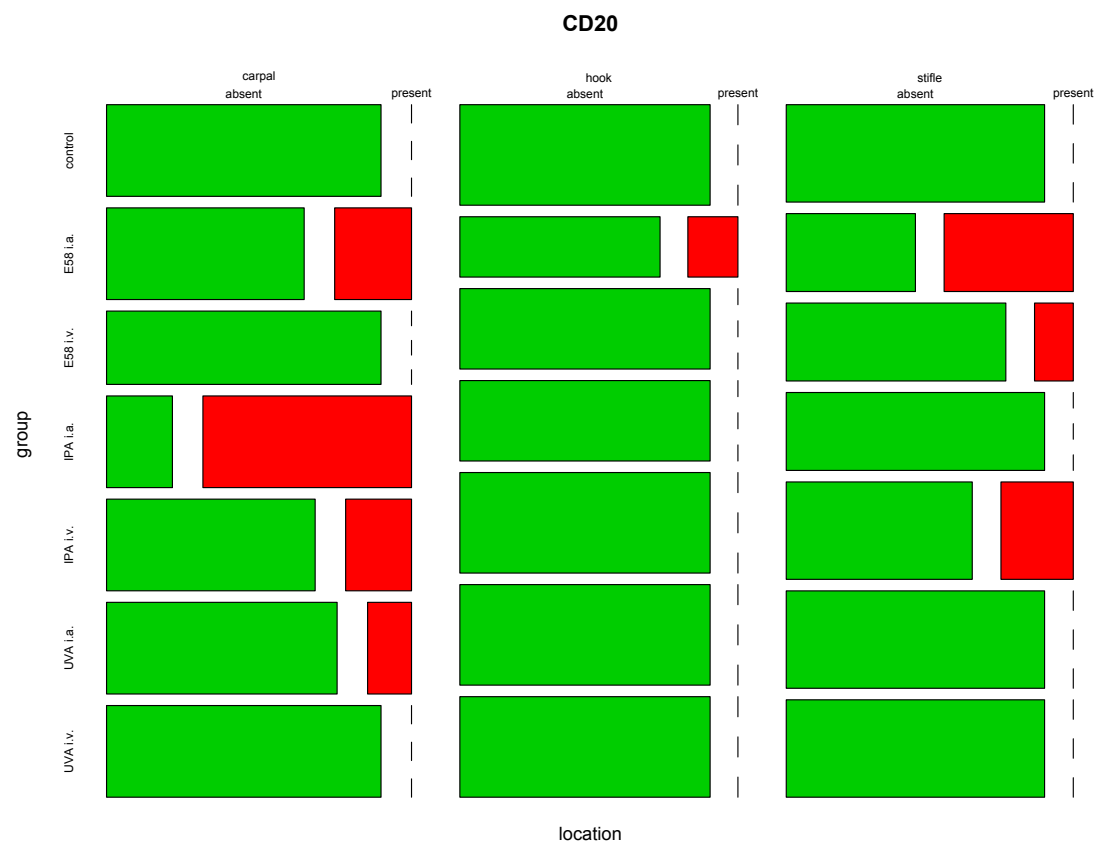
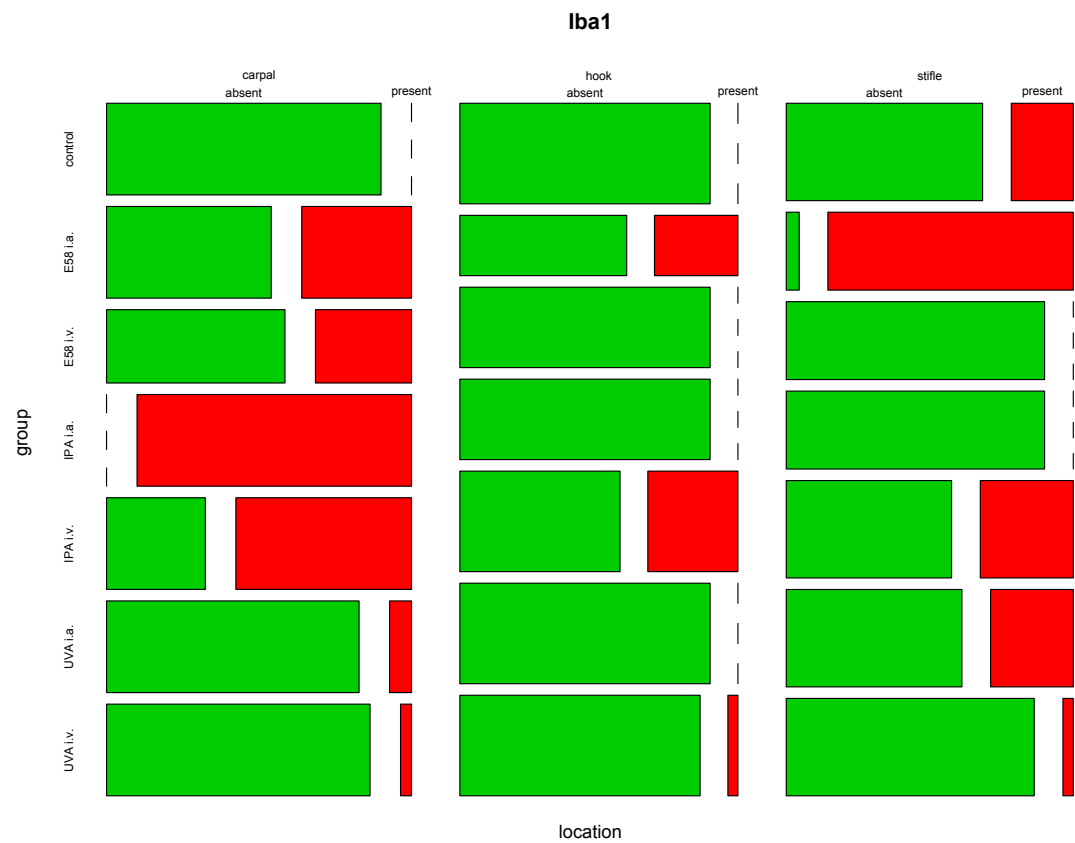


Figure 31:



Supplementary Table 1: Histopathologic joint diagnoses from experimentally *C. pecorum*- infected animals grouped according to inoculum, route of administration, qPCR, immunohistochemistry (IHC, ChIC), and total score per animal.

group	animal ID / joint	administration route	pathological- anatomical diagnosis (HE) <sup>a</sup>	qPCR (copies/ul)	IHC (ChIC) <sup>b</sup>	total score/ animal
control	351/ carpal	i.a. <sup>c</sup>	np <sup>d</sup>	0	neg <sup>e</sup>	0
	351/ hock			0		
	351/ stifle			0		
	655/ carpal			0		
	655/ hock		np <sup>d</sup>	0	neg <sup>e</sup>	3
	655/ stifle			0		
	356/ carpal			0		
	356/ hock			0		
	356/ stifle		moderate chronic focal lymphohistiocytic peri-arthritis' (possibly Injection site- induced)	0		
	687/ carpal			0		
	687/ hock			0		
	687/ stifle			0		
	373/ carpal		np <sup>d</sup>	0	neg <sup>e</sup>	0
	373/ hock			0		
	373/ stifle		np <sup>d</sup>	0	neg <sup>e</sup>	0
<i>C. pecorum</i> UV- IPA <sup>h</sup>	396/ carpal	i.a. <sup>c</sup>	np <sup>d</sup>	0	neg <sup>e</sup>	0
	396/ hock			0		
	396/ stifle			0		
	568/ carpal			0		
	568/ hock		mild acute focal purulent fibrillitis	0	neg <sup>e</sup>	1
	568/ stifle			0		
	595/ carpal			0		
	595/ hock			0		
	595/ stifle		np <sup>d</sup>	0		0
	394/ carpal			0		
	394/ hock			0		
	394/ stifle			0		
	544/ carpal		mild chronic multifocal lymphoplasmahistiocytic synovitis <sup>g</sup>	0	neg <sup>e</sup>	2
	544/ hock			0		
	544/ stifle			0		
	393/ carpal			0		
	393/ hock		moderate chronic- active multifocal lymphoplasmahistiocytic and purulent arthritis' and synovitis <sup>g</sup>	0	neg <sup>e</sup>	7
	393/ stifle			0		
	671/ carpal			0		
	671/ hock			0		
	671/ stifle		mild acute focal purulent cellulitis with mild focal haemorrhage	0	neg <sup>e</sup>	4
	681/ carpal			0		
	681/ hock			0		
	681/ stifle			0		
	681/ carpal	i.v. <sup>j</sup>	mild chronic multifocal lymphohistiocytic synovitis <sup>g</sup>	0	neg <sup>e</sup>	2
	681/ hock			0		
	681/ stifle			0		
	681/ carpal			0		

<b>C. pecorum</b> IPA <sup>k</sup>	685/ carpal		mild chronic multifocal lymphohistiocytic synovitis <sup>g</sup>	0	neg <sup>e</sup>	2
	685/ hock		np <sup>d</sup>	0		
	685/ stifle			0		
	604/ carpal		np <sup>d</sup>	0	neg <sup>e</sup>	0
	604/ hock			0		
	604/ stifle			0		
	716/ carpal	i.a. <sup>c</sup>	np <sup>d</sup>	113278	neg <sup>e</sup>	12
	716/ hock			0		
	716/ stifle		severe chronic- active multifocal lymphoplasmahistiocytic and purulent arthritis <sup>i</sup>	0		
	628/ carpal		severe chronic- active multifocal lymphoplasmahistiocytic and purulent arthritis <sup>i</sup>	24564	pos <sup>i</sup>	12
<b>C. pecorum</b> E58 <sup>m</sup>	628/ hock		np <sup>d</sup>	0	neg <sup>e</sup>	
	628/ stifle			0		
	661/ carpal		np <sup>d</sup>	178342	neg <sup>e</sup>	13
	661/ hock			0		
	661/ stifle		severe chronic- active multifocal lymphoplasmahistiocytic and purulent arthritis <sup>i</sup> and synovitis <sup>g</sup>	71		
	578/ carpal		moderate chronic- active multifocal lymphoplasmacelluar and purulent arthritis <sup>i</sup> and synovitis <sup>g</sup>	83619	neg <sup>e</sup>	23
	578/ hock		tissues missing	0		
	578/ stifle		moderate chronic- active multifocal lymphoplasmacelluar and purulent arthritis <sup>i</sup> and synovitis <sup>g</sup>	0		
	723/ carpal		moderate chronic multifocal lymphoplasmacelluar arthritis <sup>i</sup> and synovitis <sup>g</sup>	142313	neg <sup>e</sup>	6
	723/ hock		tissues missing	3532		
	723/ stifle			3067		
	658/ carpal	i.v. <sup>j</sup>	mild chronic- active diffuse lymphoplasmahistiocytic arthritis <sup>i</sup>	8192	neg <sup>e</sup>	24
	658/ hock		np <sup>d</sup>	361		
	658/ stifle		severe chronic- active lymphocytic and purulent diffuse arthritis <sup>i</sup>	2342	pos <sup>i</sup>	
	616/ carpal		moderate chronic diffuse lymphocytic arthritis <sup>i</sup> with mild acute focal purulent synovitis <sup>g</sup>	0	neg <sup>e</sup>	21
	616/ hock		mild chronic- active lymphocytic and purulent focal synovitis <sup>g</sup>	347		
	616/ stifle		mild chronic focal lymphoplasmacelluar arthritis <sup>i</sup> with mild chronic- active focal lymphoplasmacelluar and purulent synovitis <sup>g</sup>	467		
	335/ carpal		moderate chronic multifocal lymphohistiocytic arthritis <sup>i</sup>	0	neg <sup>e</sup>	14
	335/ hock		moderate chronic multifocal lymphohistiocytic arthritis <sup>i</sup> and synovitis <sup>g</sup>	365		
	335/ stifle		tissues missing	524		
	320/ carpal		mild chronic multifocal lymphoplasmahistiocytic arthritis <sup>i</sup> and synovitis <sup>g</sup>	0	neg <sup>e</sup>	14
	320/ hock		tissues missing	130		
	320/ stifle		mild chronic multifocal lymphohistiocytic synovitis <sup>g</sup>	130		
	591/ carpal		np <sup>d</sup>	2506	neg <sup>e</sup>	6
	591/ hock		moderate chronic multifocal lymphocytic arthritis <sup>i</sup> and synovitis <sup>g</sup>	190		
	591/ stifle		mild chronic multifocal lymphoplasmacelluar synovitis <sup>g</sup>	0		
	370/ carpal	i.a. <sup>c</sup>	np <sup>d</sup>	9641	neg <sup>e</sup>	18

	370/ hock			moderate chronic multifocal lymphohistiocytic arthritis with severe chronic- active lymphohistiocytic and purulent synovitis <sup>g</sup>	0			
	370/ stifle			mild chronic- active focal lymphohistiocytic and purulent synovitis <sup>g</sup>	0			
	710/ carpal			severe chronic- active multifocal lymphoplasmahistiocytic and purulent arthritis <sup>l</sup> and moderate acute multifocal purulent synovitis <sup>g</sup>	71303		pos <sup>l</sup>	25
	710/ hock			tissues missing	0			
	710/ stifle			severe chronic- active multifocal lymphohistiocytic and purulent synovitis <sup>g</sup>	0			
	315/ carpal			severe chronic multifocal lymphoplasmahistiocytic arthritis <sup>l</sup> and moderate acute multifocal purulent synovitis <sup>g</sup>	124059		neg <sup>g</sup>	11
	315/ hock			tissues missing	0			
	315/ stifle			tissues missing	0			
	673/ carpal			severe chronic multifocal lymphoplasmahistiocytic arthritis <sup>l</sup> and synovitis <sup>g</sup>	167349		neg <sup>g</sup>	7
	673/ hock			npf <sup>fl</sup>	0		neg <sup>g</sup>	
	673/ stifle				0			
	328/ carpal			severe chronic multifocal lymphoplasmahistiocytic arthritis <sup>l</sup>	87848		neg <sup>g</sup>	13
	328/ hock			moderate acute multifocal purulent synovitis <sup>g</sup>	0			
	328/ stifle			npf <sup>fl</sup>	0			
	365/ carpal		i.v. <sup>l</sup>	moderate chronic focal lymphohistiocytic arthritis <sup>l</sup>	0		neg <sup>g</sup>	3
	365/ hock			npf <sup>fl</sup>	92			
	365/ stifle			mild chronic multifocal lymphoplasmahistiocytic synovitis <sup>g</sup>	0			
	593/ carpal			moderate chronic multifocal lymphohistiocytic synovitis <sup>g</sup>	1884		neg <sup>g</sup>	7
	593/ hock			npf <sup>fl</sup>	421			
	593/ stifle			mild acute focal purulent synovitis <sup>g</sup>	0			
	339/ carpal			tissues missing	0		neg <sup>g</sup>	n/a
	339/ hock				337			
	339/ stifle				419			
	694/ carpal			npf <sup>fl</sup>	251		neg <sup>g</sup>	8
	694/ hock				0			
	694/ stifle			mild to moderate acute multifocal purulent and mild chronic focal lymphohistiocytic arthritis <sup>l</sup>	347			
	531/ carpal			npf <sup>fl</sup>	0		neg <sup>g</sup>	0
	531/ hock				488			
	531/ stifle				0			

<sup>fl</sup>HE = hematoxylin and eosin staining

<sup>fl</sup>HC = immunohistochemistry for chlamydial antigen (CHC).

<sup>fl</sup>IA = intraarticular (administration in carpal joint or right front leg).

<sup>fl</sup>PI = no pathological findings.

<sup>fl</sup>neg = negative.

<sup>fl</sup>periditis: area around joint inflamed.

<sup>fl</sup>synovitis: synovial membrane inflamed.

<sup>fl</sup>C.pecorum UV: irradiated.

<sup>fl</sup>arthritis: joint inflamed.

<sup>fl</sup>I.v. = intravenous (administration in jugular vein).

<sup>fl</sup>C. pecorum: strain IFA.

<sup>fl</sup>pos= positive.

<sup>fl</sup>C. pecorum: strain E58.



**Supplementary Table 2: Histopathologic diagnoses of joints and inner organs from naturally *C. pecorum*- infected animals, qPCR, chlamydial immunohistochemistry (IHC, ChIC), and total score per animal.**

animal ID/ organ	Histopathologic diagnosis (HE) <sup>a</sup>	qPCR (copies/μl)	IHC (ChIC) <sup>b</sup>	score/ animal
3619, lung	np <sup>f</sup>	n/a <sup>d</sup>	negative	51
3619, liver	mild chronic focal lymphocytic periportal hepatitis			
3619, spleen	np <sup>f</sup>			
3619, kidney	moderate to severe chronic multifocal lymphoplasmacellular pyelitis, mildly ascending into the papilla			
3619, lymphnode	np <sup>f</sup>			
3619, conjunctiva	severe chronic- active multifocal lymphoplasmacellular and purulent conjunctivitis with follicle formation			32
3619, left carpal joint	moderate to severe chronic multifocal lymphoplasmacellular arthritis and chronic-active multifocal lymphoplasmacellular and purulent synovitis (mainly perivascular)	BDL <sup>e</sup>	positive	
3619, right carpal joint	moderate to severe chronic multifocal lymphoplasmacellular arthritis and chronic-active multifocal lymphoplasmacellular and purulent synovitis (mainly perivascular)	9.31	positive	
3619, right stifle joint	mild to moderate active multifocal purulent synovitis and mild chronic multifocal lymphoplasmacytic arthritis	163	negative	
8452, lung	np <sup>f</sup>	n/a <sup>d</sup>	negative	
8452, liver	mild chronic multifocal lymphocytic periportal hepatitis			30
8452, spleen	np <sup>f</sup>			
8452, kidney	np <sup>f</sup>		positive	
8452, lymphnode	np <sup>f</sup>		negative	
8452, left carpal joint	moderate to severe chronic multifocal plasmacellular arthritis and chronic-active multifocal plasmacellular and purulent synovitis (mainly perivascular)	BDL <sup>e</sup>	negative	
8452, right carpal joint	moderate chronic multifocal lymphoplasmahistiocytic arthritis and synovitis (esp. perivascular) and mild acute multifocal purulent synovitis	BDL <sup>e</sup>		15
7578, lung	np <sup>f</sup>	n/a <sup>d</sup>	negative	
7578, liver	mild chronic multifocal lymphocytic periportal hepatitis			
7578, spleen	np <sup>f</sup>			
7578, kidney	mild chronic-active focal lymphocytic and purulent pyelitis		positive	
7578, lymphnode	np <sup>f</sup>		negative	30
7578, left carpal joint	mild chronic multifocal lymphohistiocytic arthritis	34		
7578, right carpal joint	mild to moderate chronic multifocal lymphohistiocytic arthritis	BDL <sup>e</sup>	positive	
7629, lung	np <sup>f</sup>	n/a <sup>d</sup>	negative	
7629, liver	mild to moderate chronic multifocal lymphocytic periportal hepatitis			
7629, spleen	np <sup>f</sup>			15
7629, kidney	mild chronic multifocal lymphocytic pyelitis			
7629, lymphnode	np <sup>f</sup>			
7629, left carpal joint	mild to moderate chronic-active multifocal purulent and lymphocytic arthritis and mild chronic multifocal synovitis	6.76	positive	

7629, right carpal joint	np <sup>c</sup>		BDL <sup>e</sup>	negative	
8084, lung	np <sup>c</sup>		n/a <sup>d</sup>	negative	27
8084, liver	mild chronic multifocal lymphocytic periportal hepatitis				
8084, kidney	moderate to severe chronic-active multifocal lymphohistiocytic and purulent pyelitis, mildly ascending into the papilla				
8084, lymphnode	np <sup>c</sup>				
8084, left carpal joint	mild to moderate chronic-active multifocal lymphohistiocytic and purulent arthritis and synovitis		BDL <sup>e</sup>		
8084, right carpal joint	mild to moderate chronic multifocal lymphoplasmahistiocytic arthritis		BDL <sup>e</sup>	positive	

<sup>a</sup>HE = hematoxylin and eosin staining.

<sup>b</sup>IHC = immunohistochemistry for chlamydial antigen (ChIC).

<sup>c</sup>no pathologic findings.

<sup>d</sup>na= analysis was not applicable.

<sup>e</sup>BDL=below detection limit, but HRM (= High Resolution Melting Analysis) was present.

Supplementary Table 3: Histopathologic diagnoses of inner organs from experimentally *C. pecorum*-infected animals per group, route of administration, qPCR, chlamydial immunohistochemistry (IHC, ChIC), and total score per animal.

group	animal ID / organ	administration route	histopathologic diagnosis (HE) <sup>a</sup>	qPCR (copies/μl)	IHC (ChIC) <sup>b</sup>	score/ animal
control	351/ lung	i.a. <sup>c</sup>	np <sup>d</sup>	0	neg <sup>e</sup>	4
	351/ lnn			0		
	351/ brain			0		
	351/ kidney			0		
	351/ spleen		np <sup>d</sup>	0		
	351/ liver			0		
	655/ lung			0		
	655/ lnn			0	neg <sup>e</sup>	1
	655/ brain			0		
	655/ kidney			0		
	655/ spleen			0		
	655/ liver		mild focal chronic lymphocytic periportal hepatitis	0	neg <sup>e</sup>	0
	356/ lungs			0		
	356/ lnn			0		
	356/ brain			0		
	356/ kidney			0		
	356/ spleen		np <sup>d</sup>	0		
	356/ liver			0		
	687/ lungs			0	neg <sup>e</sup>	1
	687/ lnn			0		
	687/ brain			0		
	687/ kidney			0		
UV-IPA <sup>f</sup>	687/ spleen	i.a. <sup>c</sup>	leukocytostasis	0	neg <sup>e</sup>	0
	687/ liver			0		
	373/ lungs			0		
	373/ lnn		np <sup>d</sup>	0	neg <sup>e</sup>	0
	373/ brain			0		
	373/ kidney			0		
	373/ spleen			0		
	373/ liver		np <sup>d</sup>	0	neg <sup>e</sup>	2
	396/ lung			0		
	396/ lnn			0		
	396/ brain			0		
	396/ kidney			0		
	396/ spleen			0		
	396/ liver			0	neg <sup>e</sup>	1
	568/ lung		mild multifocal chronic lymphocytic periportal hepatitis	0		
	568/ lnn			0		
	568/ brain			0		



	604/ lung		leucocytostasis npf <sup>d</sup>	0	neg <sup>e</sup>	2
	604/ lnn			0		
	604/ brain			0		
	604/ kidney			0		
	604/ spleen			0		
	604/ liver			0		
	604/ liver			0		
<b>C. pecorum IPA<sup>h</sup></b>	716/ lung	i.a. <sup>c</sup>	mild chronic multifocal lymphocytic periportal hepatitis npf <sup>d</sup>	0	neg <sup>e</sup>	6
	716/ lnn			0		
	716/ brain			0		
	716/ kidney			0		
	716/ spleen			137		
	716/ liver			193		
	628/ lung		mild chronic multifocal lymphohistiocytic pyelitis npf <sup>d</sup>	212		3
	628/ lnn			0		
	628/ brain			0		
	628/ kidney			0		
	628/ spleen			0		
	628/ liver		mild acute multifocal neutrophilic periportal hepatitis npf	0	neg <sup>e</sup>	3
	661/ lung			0		
	661/ lnn			315		
	661/ brain			0		
	661/ kidney			158		
	661/ spleen		leucocytostasis npf	0	neg <sup>e</sup>	0
	661/ liver			0		
	578/ lung			0		
	578/ lnn			315		
	578/ brain			877		
<b>C. pecorum IPA<sup>h</sup></b>	578/ kidney	i.v. <sup>g</sup>	moderate chronic multifocal lymphohistiocytic meningoencephalitis focal glia nodule severe chronic-active multifocal purulent and lymphoplasmahistiocytic pyelitis, slightly ascending into the papilla mild chronic-active multifocal perivascular lymphocytic and purulent nephritis with fibrosis npf <sup>d</sup>	0	neg <sup>e</sup>	16
	578/ spleen			0		
	578/ liver			0		
	723/ lung			0		
	723/ lnn			614		
	723/ brain			0		
	723/ kidney			0		
	723/ spleen			0		
	723/ liver			0		
	658/ lung			168		
	658/ lnn			912		
	658/ brain			387		
	658/ kidney			266		
	658/ spleen			778		

	658/ liver	mild hepatolipidosis leukocytostasis	2344			
	616/ lung	severe chronic- active multifocal purulent and lymphoplasmahistiocytic pyelitis with follicle formation, ascending to the papilla moderate chronic- active focal lymphohistiocytic and purulent interstitial nephritis (neutrophils in the tubules- lumina, tubules are activated and partially degenerated)	0	neg <sup>a</sup>	17	
	616/ lnn		2087			
	616/ brain		652			
	616/ kidney		170	focal: positive		
	616/ spleen	np <sup>d</sup>	0	neg <sup>a</sup>		
	616/ liver	mild chronic multifocal lymphocytic periportal hepatitis mild multifocal hepatolipidosis	716			
	335/ lung	severe chronic- active multifocal purulent and lymphohistiocytic pyelitis with follicle formation, ascending into the papilla moderate chronic focal lymphocytic interstitial nephritis	0	neg <sup>a</sup>	12	
	335/ lnn		694			
	335/ brain		0			
	335/ kidney		865			
	355/ spleen	np <sup>d</sup>	622			
	335/ liver		0			
	320/ lung	np <sup>d</sup>	0	neg <sup>a</sup>	3	
	320/ lnn		362			
	320/ brain		0			
	320/ kidney	mild chronic multifocal lymphocytic pyelitis	0			
	320/ spleen	np <sup>d</sup>	276			
	320/ liver	leucocytostasis mild multifocal hepatolipidosis	245			
	591/ lung	np <sup>d</sup>	0	neg <sup>a</sup>	6	
	591/ lnn		0			
	591/ brain	mild chronic multifocal lymphohistiocytic meningoencephalitis	350			
	591/ kidney	np <sup>d</sup>	347			
	591/ spleen		0			
	591/ liver	leukocytostasis	103			
C. pecorum E 58 <sup>i</sup>	328/ lung	mild to moderate chronic multifocal lymphoplasmacellular periportal hepatitis				
	328/ lnn	np <sup>f</sup>	681	neg <sup>a</sup>	2	
	328/ brain		0			
	328/ kidney		882			
	328/ kidney	mild chronic focal lymphocytic interstitial nephritis (renal pelvis partially missing)	0			
	328/ spleen	np <sup>d</sup>	0			
	328/ liver		610			
	370/ lung	np <sup>d</sup>	200	neg <sup>a</sup>	2	
	370/ lnn		0			
	370/ brain		0			
	370/ kidney	mild chronic multifocal lymphoplasmacellular pyelitis	671			
	370/ spleen	np <sup>d</sup>	0			

C. <i>pecorum</i> E 58 <sup>a</sup>	370/ liver		np <sup>d</sup>	116	neg <sup>e</sup>	3
	710/ lung			0		
	710/ lnn			0		
	710/ brain			0		
	710/ kidney			0		
	710/ spleen			0		
	710/ liver			0		
	315/ lung			0		15
	315/ lnn			0		
	315/ brain			0		
	315/ kidney			0		
	315/ spleen			147		
	315/ liver			0	neg <sup>e</sup>	3
	673/ lung			0		
	673/ lnn			1045		
	673/ brain			341		
	673/ kidney			0		
	673/ spleen			0	neg <sup>e</sup>	4
	673/ liver			0		
	694/ lung	i, v. <sup>g</sup>	np <sup>d</sup>	116		
	694/ lnn			0		
	694/ brain			0		
	694/ kidney			0		
	694/ spleen			0		
	694/ liver			2136		
	365/ lung			232		
	365/ lnn			137		
	365/ brain			918		
	365/ kidney			0		
	365/ spleen			0		
	365/ liver			721		
	593/ lung			0	neg <sup>e</sup>	0
	593/ lnn			0		
	593/ brain			565		
	593/ kidney			0		
	593/ spleen			803		
	593/ liver			0	neg <sup>e</sup>	3
	339/ lung			0		
	339/ lnn			0		
	339/ brain			825		
	339/ kidney			0		
	339/ spleen			0		





Supplementary Table 4: results of the descriptive analysis (mean/median/sd) (standard derivation) of joints (carpal, hock, stiffl) and inner organs (kidney, brain, lung, lymphnodes, spleen) of experimentally infected animals including qPCR data.

score_joints	carpal, median/mean/sd: 0.00/ 3.23/ 4.50	hock, median/mean/sd: 0.00/ 1.35/ 2.93	stifle, median/mean/sd: 1.00/ 3.34/ 4.51
score_joints per group	control median/mean/sd: 0.00/ 0.40/ 1.06	UVA i.a. median/mean/sd: 0.00/ 0.53/ 1.36	IPA i.a. median/mean/sd: 0.00/ 5.08/ 5.94
score_per organ	brain: 0.00/ 0.66/ 1.21	kidney: 0.00/ 2.17/ 4.25	IPA i.v. median/mean/sd: 6.00/ 5.27/ 3.71
score organs (brain+ kidney) per group	control 0.00/ 0.20/ 0.63	UVA i.a. 0.00/ 0.20/ 0.63	IPA i.v. 2.50/ 4.80/ 5.37
lung: score_peribronchial accumulation per group	control 0.00/ 1.40/ 1.52	UVA i.a. 0.00/ 1.80/ 1.30	IPA i.v. 0.00/ 2.00/ 0.70
lung: score_peribronchial lymphfollicles per group	control 3.00/ 3.60/ 1.95	UVA i.v. 3.00/ 3.60/ 1.82	IPA i.v. 5.00/ 5.20/ 1.30
lymphnode: score_follicles per group	control 0.01/ 0.01/ 0.01	UVA i.a. 0.02/ 0.02/ 0.01	IPA i.v. 0.01/ 0.01/ 0.01
lymphnodes: score_secondary follicles per group	control 0.02/ 0.02/ 0.01	UVA i.v. 0.02/ 0.02/ 0.01	IPA i.v. 0.01/ 0.01/ 0.02
spleen: score_follicles per group	control 0.01/ 0.02/ 0.02	UVA i.a. 0.01/ 0.02/ 0.01	IPA i.v. 0.01/ 0.01/ 0.01
spleen: score_secondary follicles per group	control 0.01/ 0.01/ 0.02	UVA i.v. 0.01/ 0.01/ 0.01	IPA i.v. 0.01/ 0.01/ 0.01
joints: qPCR (copies/µl) per joint	carpal 8916.50/ 50757.45/ 63795.55	hock 46.00/ 313.15/ 777.59	stifle 0.00/ 368.35/ 826.80
joints: qPCR (copies/µl) per group	E58 i.a. 0/ 30680.00/ 54884.12	IPA i.a. 71/ 36585.73/ 61196.66	IPA i.v. 3471/ 1036.93/ 2132.94
load per carpal joint and group	E58 i.v. 59020.00/ 92040.00/ 59020.87	IPA i.v. 0.00/ 427.00/ 821.71	IPA i.v. 0.00/ 2139.60/ 3553.15
load per hock joint and group	E58 i.a. 0.00/ 0.00/ 0.00	IPA i.a. 0.00/ 706.40/ 1579.56	IPA i.v. 347.00/ 278.60/ 110.53
load per stiffl joint and group	E58 i.a. 0.00/ 0.00/ 0.00	IPA i.a. 0.00/ 153.20/ 211.32	IPA i.v. 467.00/ 692.60/ 948.16
inner organs: qPCR (copies/µl) per organ	brain 170.50/ 323.90/ 367.70	liver 0.00/ 359.20/ 688.34	spleen 0.00/ 138.15/ 268.70

inner organs: qPCR (copies/μl) per group	E58 i.a. 0.00/ 156.43/ 300.19	E58 i.v. 0.00/ 319.20/ 493.89	IPA i.a. 0.00/ 94.03/ 203.86	IPA i.v. 255.5/ 411.47/ 574.18
load per brain and group	E58 i.a. 0.00/ 244.60/ 385.70	E58 i.v. 681.00/ 597.80/ 360.39	IPA i.a. 0.00/ 175.40/ 392.21	IPA i.v. 350.00/ 277.80/ 279.06
load per kidney and group	E58 i.a. 0.00/ 134.20/ 300.08	E58 i.v. 0.00/ 187.20/ 418.59	IPA i.a. 0.00/ 31.60/ 70.66	IPA i.v. 266.00/ 329.60/ 326.00
load per liver and group	E58 i.a. 0.00/ 145.20/ 264.64	E58 i.v. 0.00/ 571.40/ 928.69	IPA i.a. 0.00/ 38.60/ 86.31	IPA i.v. 245.00/ 681.60/ 968.86
load per lymphnode and group	E58 i.a. 0.00/ 209.00/ 467.34	E58 i.v. 0.00/ 174.00/ 318.07	IPA i.a. 315.00/ 248.80/ 257.85	IPA i.v. 694.00/ 811.00/ 792.37
load per lung and group	E58 i.a. 0.00/ 176.20/ 295.18	E58 i.v. 116.00/ 224.20/ 321.51	IPA i.a. 0.00/ 42.40/ 94.81	IPA i.v. 0.00/ 33.60/ 75.13
load per spleen and group	E58 i.a. n/a	E58 i.v. n/a	IPA i.a. n/a	IPA i.v. n/a

Supplementary Table 5: Statistical results obtained from mixed effect models ( effect sizes and 95% confidence intervals, p-values, p- value) of joints (carpal, hock, stifle), inner organs (kidney, brain, lung, lymphnodes, spleen), biomarker and qPCR values. Assessment and comparison of experimental groups compared to the control group.

score_joints per group	UVA i.a. confidence interval/ p- value	UVA i.v. confidence interval/ p-value	E58 i.a.: confidence interval/ p-value	E58 i.v. confidence interval/ p-value	IPA i.a. confidence interval/ p-value	IPA i.v. confidence interval/ p-value
score organs (brain+ kidney) per group	UVA i.a. 2.28 (-3.24 to 3.24) / 1.00	UVA i.v.: -1.00 (-3.34 to 3.14) / 1.00	E58 i.a.: 1.50 (-1.74 to 4.74) / 0.69	E58 i.v.: 1.90 (-1.34 to 5.14) / 0.46	IPA i.a. 2.60 (1.29 to 3.90) / 0.001	IPA i.v. 2.61 (1.32 to 3.90) / 0.001
lung: score_peribron chial accumulation per group	UVA i.a. 0.40 (-2.21 to 3.01) / 0.91	UVA i.v.: -0.20 (-2.81 to 2.4) / 0.91	E58 i.a.: -0.80 (-3.41 to 1.81) / 0.91	E58 i.v.: -0.80 (-3.41 to 1.81) / 0.97	IPA i.a. 6.00 (-2.64 to 3.84) / 0.99	IPA i.v. 4.69 (1.36 to 7.84) / 0.01
lung: score_peribron chial lymphfollicles per group	UVA i.a. 1.60 (-1.69 to 4.89) / 0.10	UVA i.v.: -1.10 (-3.29 to 3.29) / 1.00	E58 i.a. -4.00 (-3.89 to 2.89) / 0.10	E58 i.v. 2.00 (-3.09 to 3.49) / 0.60	IPA i.a. -6.00 (-3.89 to 2.69) / 1.00	IPA i.v. 1.60 (-1.69 to 4.89) / 0.60
lymphnode: score_follicles per group	UVA i.a. 0.01 (-0.01 to 0.03) / 0.34	UVA i.v.: 0.01 (-0.01 to 0.03) / 0.51	E58 i.a. 0.00 (-0.02 to 0.02) / 0.10	E58 i.v. 0.02 (-0.00 to 0.03) / 0.08	IPA i.a. 0.00 (-0.01 to 0.02) / 0.10	IPA i.v. 0.00 (-0.01 to 0.02) / 0.95
lymphnodes: score_seconda ry follicles per group	UVA i.a. -0.00 (-0.02 to 0.02) / 1.00	UVA i.v.: 0.01 (-0.01 to 0.03) / 0.93	E58 i.a. -0.01 (-0.03 to 0.01) / 0.90	E58 i.v. 0.01 (-0.01 to 0.03) / 0.60	IPA i.a. -0.00 (-0.02 to 0.02) / 1.00	IPA i.v. -0.00 (-0.02 to 0.02) / 0.10
spleen: score_follicles per group	UVA i.a. -0.00 (-0.02 to 0.01) / 0.99	UVA i.v.: -0.01 (-0.03 to 0.01) / 0.54	E58 i.a. -0.01 (-0.03 to 0.01) / 0.66	E58 i.v. -0.01 (-0.02 to 0.01) / 0.78	IPA i.a. -0.00 (-0.02 to 0.01) / 0.97	IPA i.v. -0.01 (-0.03 to 0.01) / 0.68
spleen: score_seconda ry follicles per group	UVA i.a. 0.00 (-0.03 to 0.03) / 1.00	UVA i.v.: -0.00 (-0.03 to 0.03) / 1.00	E58 i.a. -0.00 (-0.03 to 0.02) / 0.10	E58 i.v. 0.01 (-0.02 to 0.04) / 0.10	IPA i.a. 0.01 (-0.02 to 0.04) / 0.77	IPA i.v. -0.00 (-0.03 to 0.02) / 0.10
hock score_CD3 per joint	1.85 (-2.40 to 1.43) / 0.001	hock score_CD3 per joint	stifle 3.78 (1.77 to 8.08) / 0.01	stifle 3.78 (1.77 to 8.08) / 0.01	stifle 3.78 (1.77 to 8.08) / 0.01	stifle 3.78 (1.77 to 8.08) / 0.01
score_CD3 per group	UVA i.a. 1.00 (1.10 to 5.02) / 1.00	UVA i.v.: 1.20 (3.13 to 4.62) / 0.001	E58 i.a. 6.33 (1.83 to 2.19) / 0.004	E58 i.v. 3.10 (4.11 to 3.88) / 0.43	IPA i.a. 1.15 (3.40 to 3.89) / 0.001	IPA i.v. 8.44 (2.36 to 3.02) / 0.001
score_CD3 per area	1.0 (8.17 to 1.22) / 1.00	1.0 (8.17 to 1.22) / 1.00	stifle 0.48 (0.23 to 0.10) / 0.05	stifle 0.48 (0.23 to 0.10) / 0.05	stifle 0.48 (0.23 to 0.10) / 0.05	stifle 0.48 (0.23 to 0.10) / 0.05
score_CD20 per joint	hock 0.06 (0.02 to 0.20) / 0.001	hock 0.06 (0.02 to 0.20) / 0.001	stifle 0.48 (0.23 to 0.10) / 0.05	stifle 0.48 (0.23 to 0.10) / 0.05	stifle 0.48 (0.23 to 0.10) / 0.05	stifle 0.48 (0.23 to 0.10) / 0.05
score_CD20 per group	UVA i.a. 4.27 (0.48 to 37.90) / 0.19	UVA i.v.: 1.00 (0.06 to 15.64) / 1.00	E58 i.a. 38.58 (5.35 to 278.26) / 0.001	E58 i.v. 3.98 (0.42 to 37.44) / 0.23	IPA i.a. 34.49 (4.75 to 250.48) / 0.001	IPA i.v. 17.30 (2.20 to 135.68) / 0.01

score_CD20 per area	0.90 (0.73 to 1.10) / 0.30					
score_lba1 per joint	hock 0.16 (0.08 to 0.32) / 0.001		stifle 0.63 (0.33 to 1.20) / 0.16			
score_lba1 per group	UVA i.a. 1.80 (0.69 to 4.76) / 0.23	UVA i.v. 0.47 (0.12 to 1.85) / 0.28	E58 i.a. 16.27 (6.65 to 39.78) / 0.001	E58 i.v. 1.54 (0.54 to 4.41) / 0.42	IPA i.a. 7.76 (3.49 to 17.24) / 0.001	IPA i.v. 11.39 (4.62 to 28.06) / 0.001
score_lba1 per area	0.99 (0.85 to 1.34) / 0.83					
load_qPCR per joint:	hock/ carpal: -5.09 (-5.12 to -5.06) / 0.001					
load_qPCR joint per group:	E58 i.v./ E 58 i.a. -4.80 (-6.46 to 3.14) / 0.001	IPA i.a./ E58 i.a. 0.32 (-1.34 to 1.98) / 0.96	IPA i.v./ E58 i.a. 0.32 (-1.4 to 1.98) / 0.001	IPA i.a./ E58 i.v. 5.12 (3.46 to 6.78) / 0.001	IPA i.v./ E58 i.v. 0.95 (-0.70 to 2.61) / 0.45	IPA i.v./ IPA i.a. -4.17 (-5.83 to -2.51) / 0.001
load_qPCR per organ:	Kidney n/a / 0.33	Liver n/a / 0.70	Lymphnode n/a / 0.52	Lung n/a / 0.04	Spleen n/a / 0.26	
load_qPCR per group:	E58 i.v. n/a / 0.30	IPA i.a. n/a / 0.10		IPA i.v. n/a / 0.77		

## Danksagung

An erster Stelle möchte ich mich herzlichst bei Prof. Dr. Nicole Borel für die Überlassung des Dissertationsthemas, die unermüdliche Hilfe und optimale Betreuung bedanken.

Mein weiterer Dank gilt dem Laborteam, Theresa Pesch, Barbara Prähauser und Sabina Wunderlin für die Unterstützung im Labor sowie Dr. Monika Hilbe und Dr. Titus Sydler für ihre Hilfe bei der Auswertung der Schnitte von Gehirn, Niere und Lunge.

Weiterhin danke ich Jeanne Peter für die Bearbeitung unserer Fotoplates, Dr. Sonja Hartnack für den gesamten statistischen Teil dieser Arbeit und Prof. Dr. Michael Hässig für die Übernahme des Korreferates.

Vielen Dank auch an unsere australischen Kooperationspartner Dr. Martina Jelocnik, Phd Mominul Islam, Prof. Adam Polkinghorne, Ian Marsh, Narelle Sales, Prof. Caroline Jacobson and Tom Clune.

Von Herzen danke ich meiner Familie, vor allem meinen Eltern Anne und Arno. Ihr habt immer an mich geglaubt und mir so viel ermöglicht. Grosser Dank gilt auch all meinen Freunden, welche mich bereits während des Studiums und bis jetzt in allen erdenklichen Lebenslagen unterstützt haben. Danke Anna, für den tollsten und spannendsten Umzug in die Schweiz und danke Sophie für den Import von Major. Danke an all meine im IVPZ neu gewonnenen Freunde. Ihr habt die Patho zu einer Familie gemacht.

*Und jedem Anfang wohnt ein Zauber inne, der uns beschützt und der uns hilft zu leben.*

*Hermann Hesse*

## Curriculum Vitae

Vorname Name	<b>Nina Ostfeld</b>
Geburtsdatum	24.02.1988
Geburtsort	Bremen, Deutschland
Nationalität	deutsch
07/2004- 7/2007	<b>Gymnasium</b> , Schulzentrum der Sekundarstufe II, Bremen, Deutschland
25.07.2007	<b>Matura</b> , Schulzentrum der Sekundarstufe II, Bremen, Deutschland
10/2008- 10/2010	<b>Ausbildung zur Tiermedizinischen Praxisassistentin</b> , Tierärztekammer Bremen, Tierarztpraxis Dr. med. vet. Holger Schöner, Bremen, Deutschland
10/2013- 03/2019	<b>Studium der Tiermedizin</b> , Justus- Liebig- Universität Giessen, Deutschland
08.02.2019	<b>Abschlussprüfung vet. med.</b> , Justus- Liebig- Universität Giessen, Deutschland
04/2019 – 07/2020	<b>Anfertigung der Dissertation</b> unter Leitung von Prof. Dr. med. vet. Nicole Borel am Institut für Veterinärpathologie Abteilung für Infektionspathologie der Vetsuisse-Fakultät Universität Zürich Direktorin: Prof. Dr. med. vet., Dipl.ECVP, FRCPath, FTA & FHV (Pathologie) Anja Kipar

02/2019 – 02/2020

Assistentztierärztin, Institut für Veterinärpathologie,  
Zürich, Schweiz

03/2020 – heute

Assistentztierärztin, Abteilung für  
Kleintierreproduktion, Tierspital Zürich, Schweiz